Biosafety of a 3D-printed Intraocular Lens Made of a Poly(Acrylamide-Co-Sodium Acrylate) Hydrogel *In Vitro* and *In Vivo*

Running title: Biosafety of Poly(Acrylamide-Co-Sodium Acrylate) as IOL material

Jiawen Li,[1,2] Yijian Li,[1,2] Xisu Hu, [1,2] Yu Gong,[1,2] Ben Bin Xu,[3] Haiwei Xu,[1,2] Zheng Qin Yin[1,2]

[1]Southwest Hospital/Southwest Eye Hospital, Third Military Medical University (Army Medical University), Chongqing, P.R. China

[2]Key Lab of Visual Damage and Regeneration & Restoration of Chongqing, Chongqing, P.R. China

[3]Smart Materials and Surfaces Lab, Faculty of Engineering and Environment, Northumbria University, Newcastle upon Tyne NE1 8ST, UK

Correspondence to: Haiwei Xu and Zheng Qin Yin. Southwest Hospital/Southwest Eye Hospital, Third Military Medical University (Army Medical University), Chongqing 400038, P.R. China.

E-mail addresses: xuhaiwei@tmmu.edu.cn; qinzyin@aliyun.com

Abstract

AIM: To assess the biosafety of a poly(acrylamide-co-sodium acrylate) hydrogel as a 3D-printed intraocular lens (IOL) material.

METHODS: The biosafety of the poly(acrylamide-co-sodium acrylate) hydrogel was first analyzed *in vitro* using human lens epithelial cells (LECs) and the ARPE19 cell line, and a CCK-8 assay was performed to investigate alterations in cell proliferation. A thin film of a poly(acrylamide-co-sodium acrylate) hydrogel and a conventional IOL were intraocularly implanted into the eyes of New Zealand white rabbits respectively, and a sham surgery served as control group. The anterior segment photographs, intraocular pressure (IOP), blood parameters and electroretinograms were recorded. Inflammatory cytokines in the aqueous humor, such as TNFα and IL-8, were examined by ELISA. Cell apoptosis of the retina was investigated by TUNEL assay, and macrophage activation was detected by immunostaining.

RESULTS: The poly(acrylamide-co-sodium acrylate) hydrogel did not slow cell proliferation when cocultured with human LECs or ARPE19 cells. The implantation of a thin film of a 3D-printed IOL composed of the poly(acrylamide-co-sodium acrylate) hydrogel did not affect the IOP, blood parameters, electroretinogram or optical structure in any of the three experimental groups (n=3 for each group). Both TNFα and IL-8 in the aqueous humor of the hydrogel group were transiently elevated 1 week post-operation and recovered to normal levels at 1 and 3 months post-operation. Iba1$^+$ macrophages in the anterior chamber angle of the hydrogel group were increased markedly compared to those of the control group; however, there was no significant difference compared to those in the IOL group.

CONCLUSION: The poly(acrylamide-co-sodium acrylate) hydrogel is a safe material for 3D printing of personal IOLs that hold great potential for future clinical applications.

KEYWORDS: Cataract; Biosafety; Lens Epithelial Cells; ARPE19 Cells; Intraocular Lens; 3D Printing; Poly Hydrogel; Rabbit

INTRODUCTION

More than 95 million people worldwide have cataracts, which is the leading cause of blindness.[1] Phacoemulsification combined with intraocular lens (IOL) implantation is the most effective way to treat cataract so far.[2] However, the mass-produced model IOL based on a high-precision

machine tool fails to meet the growing demands of personalized customization of the human lens, and it is hard to obtain the best postoperative vision.[3] Precision medicine is an inevitable trend in the development of clinical medicine, personalized customization is an extremely important component of precision medicine, and personalized IOL customization is an important means to improve the outcome of cataract surgery.

3D printing holds great potential in biomedical engineering research as well as in ophthalmologic applications,[4-6] which enables cost-effective products and instruments that aid in therapeutic devices, such as IOLs, built specifically for individual cataract patients.[7] Based on the clinical data, it is possible for us to design a personalized IOL suitable for the size of the lens capsule by digital optical modeling, simulating the quality of IOL imaging and correcting the wave front aberration.[8] Achievement of 3D printing of IOLs is a great challenge, and the breakthrough bottleneck lies in the following points: 1) the fabrication of ultrahigh-precision roughness of the IOL surface (micro/nano-precision);[9] 2) the high transparency and UV-blocking ability of materials; 3) the flexibility, water richness and micromechanical characteristics of the organic materials; and 4) the biosafety of the material for 3D-printed IOLs.[10,11]

Additive manufacturing and 3D printing create new approaches for the design and manufacturing of implants, such as microstructured eye implants, including multifocal diffractive aspheric IOL.[12] We planned to print the IOL mold with a new responsive poly(acrylamide-co-sodium acrylate) hydrogel with 3D precise printing technology, which aims to provide accurate and personalized IOL products for cataract patients. The gel is a fully diluted crosslinking system that has no fluidity in the stable state. The main component of the gel is liquid by weight. However, due to the 3D crosslinking network, the structural integrity of the hydrogel network will not be dissolved due to the high hydrophilicity. Hydrogels are highly absorbent and light permeable (containing more than 90% water). Due to its high water content, the hydrogel also has a very similar flexibility to natural tissue, which makes it an ideal 3D printing material for making personalized IOLs. However, as responsive smart materials, hydrogels can encapsulate chemical compounds such as glucose, which are released by the stimulation of external factors, such as changes in pH. Thus, whether a poly(acrylamide-co-sodium acrylate) hydrogel is toxic to ocular tissue needs to be deliberately considered. Nevertheless, the issue of the biosafety of poly(acrylamide-co-sodium acrylate) hydrogels is unclear so far.

Here, we utilized a poly(acrylamide-co-sodium acrylate) hydrogel to create a thin film in order to investigate its biosafety after intraocular implantation. It was demonstrated *in vivo* that IOP, ERGs and inflammatory factors in the aqueous humor exhibited no significant difference after poly(acrylamide-co-sodium acrylate) hydrogel implantation. Moreover, similar results could be verified by experiments *in vitro*. Taken together, the results indicate that the poly(acrylamide-co-sodium acrylate) hydrogel does not harm the rabbit ocular tissue and causes no inflammation *in vitro* or *in vivo*, supporting the idea that it is a safe material for on-demand manufacturing of patient-personalized IOLs.

MATERIALS AND METHODS

Laboratory Animal Welfare

All experiments were performed on New Zealand white rabbits provided by the Experimental Animal Centre of Southwest Hospital, Army Medical University. The New Zealand white rabbits were all raised in the Animal Care Centre of the Army Medical University and maintained with free access to water and food under a 12-h light/dark cycle. All animal experimental procedures

were formally approved by the Institutional Review Board of the Army Medical University.

Preparation of the Poly(Acrylamide-Co-Sodium Acrylate) Hydrogel Thin Film

The hydrogel solution was prepared according to the following formula: 17.5% N-isopropylacrylamide; 12.5% sodium acrylate; 1.5% N,N'-methylenebisacrylamide; N,N,N',N'-tetramethylethylenediamine; 10% ammonium persulfate, H_20. The solution was added to one of the molds and immediately joined with another mold. Then, the two pieces of mold were clamped together. After 30~60 minutes, after the gel was solidified, and the two molds were removed. The formed hydrogel crystals were transferred to phosphate buffered saline (PBS) for preservation.

Intraocular Implantation of the Poly(Acrylamide-Co-Sodium Acrylate) Hydrogel Thin Film into New Zealand White Rabbit Eyes

The New Zealand white rabbits were divided into three groups based on implants: the poly(acrylamide-co-sodium acrylate) hydrogel thin film as the hydrogel group, the conventional IOL as the IOL group, and the sham surgery as the control group (n=3 for each group). Animals were anesthetized with 3% pentobarbital sodium 1 ml/kg through the ear-rim auricular vein; the left eye was selected as the operative eye. Before the operation, tropicamide eye drops (Santen) were used for mydriasis. The eyelid was opened with an eye speculum, and the conjunctival sac was soaked with 5% povidone iodine for 90 seconds and then rinsed with saline. A 3.0 mm width transparent corneal incision was made at the 12 o'clock position, a 1.0 mm width auxiliary corneal incision was made at the 9 o'clock position, and sodium hyaluronate (SINGCLEAN) was injected into the anterior chamber. For the control group, the incision was sutured directly with 10-0 polypropylene. For the hydrogel group and IOL group, we performed capsulorhexis, water separation, and phacoemulsification of the lens nucleus (Laureate, Alcon, USA), cleared the lens cortex with I/A, and injected the poly(acrylamide-co-sodium acrylate) hydrogel thin film (5 mm×5 mm) or IOL (860 UV, acrylic intraocular lenses as a positive control of biosafety). The 12 o'clock incision was sutured with 10-0 nylon suture, balanced salt solution (BSS) was injected to form the anterior chamber capacity, and tobramycin dexamethasone eye ointment (Alcon, USA) was applied to the eyes after the operation. Intraocular pressures (IOP) was measured by a noncontact tonometer at 1 day, 1 week, 1 month, and 3 months post-operation.

Euthanasia and Histopathology

Three months after implantation, the New Zealand white rabbits were euthanized with pentobarbital sodium (400 mg/kg) administered intravenously. Afterwards, each eye containing the implant was taken from each rabbit for histological examination. Specimens were fixed in 4% paraformaldehyde for at least 24 hours and dehydrated in 30% sucrose for at least 24 hours, followed by embedding with Tissue-Tek O.C.T. Compound (Sakura Finetek USA, Inc., Torrance, CA 90501, USA). All tissue pieces were cut into 2–4 μm thick tissue sections (Leica CM1900UV cryostat). Then, all sections were routinely stained with hematoxylin-eosin (HE) and examined under a light microscope (OLYMPUS DP71; Olympus Europa SE & Co. KG, Hamburg, Germany) to assess fibroblast proliferation and anatomical abnormalities.

Cell Culture

Human lens epithelial cells (LECs) were expanded from lens explants, which were provided by the Southwest Hospital Eye Bank. Briefly, the lens was washed in cold PBS containing 50 U mL^{-1} penicillin and 100 μg mL^{-1} streptomycin, cut into 5 mm×5 mm small pieces and seeded onto human vitronectin (Gibco, Thermo Fisher, USA) precoated plates, and the explants were left for attachment. The second day, LECs were cultured in conditioned medium consisting of DMEM/F12 (HyClone), 10% FBS (Gibco), insulin-transferrin sodium selenite (1 μg mL^{-1}, Gibco), penicillin (100 U mL^{-1}) and streptomycin (100 μg mL^{-1}, HyClone). As cells reached subconfluence, they were gently passaged at 1:6 to expand. The ARPE19 cell line was cultured according to the same procedures and conditions described above. The cells were co-cultured with the poly(acrylamide-co-sodium acrylate) hydrogel thin film (5 mm×5 mm) or PBS as control.

Immunostaining to Identify LECs

Immunostaining was routinely performed as previously described.[13] Sections were incubated for 15 minutes with PBS, and sections were further incubated with PBS containing 0.1% (vol/vol) Triton X-100 for 15 minutes and further blocked with 1% (wt/vol) bovine serum albumin (BSA) in PBS at room temperature. The following primary antibodies were incubated at 4℃ overnight: Pax6 (1:500, Abcam), Sox2 (1:400, Abcam), αA-crystallin (1:200, Santa Cruz), α-SMA (1:400, Abcam), and Iba1 (1:500, Wako).

TUNEL Staining to Analyze the Apoptotic Cells and Immuno Cells in the Eyes Of Rabbits

Using the TUNEL Assay Kit (Abcam) as previously described[14], the secondary antibodies included the goat anti-mouse Alexa Fluor 488 and goat anti-mouse Alexa Fluor 594 (Invitrogen). DAPI (1:10, Beyotime) was incubated for 8-10 minutes at 20℃ to counterstain nuclei, followed by cover-slipping with antifade mounting medium (Beyotime).

CCK-8 Assay to Analyze the Proliferation of LECs and APRE19 Cells

The cytotoxicity of the poly(acrylamide-co-sodium acrylate) hydrogel was measured using the Cell Counting Kit-8 (CCK-8) assay according to a previously published protocol.[15] Absorbance at wavelengths of 450 and 650 nm was collected using a microplate reader (Varioskan Flash, Thermo Fisher, USA).

ELISA Assay to Analyze Cytokines

The aqueous humor was extracted with a 30G sterile needle syringe at the 9 o'clock position of the limbus at 1 week, 1 month, and 3 months post-operation. ELISAs to detect IL-8 and TNF (cloud-clone corp.) were performed as previously reported.[16] The absorbance of each well was read at 450 nm and 550 nm. The 550 nm values were subtracted from the 450 nm values to correct for optical imperfections in the microplate.

Electroretinogram Recording to Assess The Visual Function of Rabbits

Scotopic flash electroretinogram recording was performed at 3 months post-operation as described previously.[17] Briefly, after 12-h dark adaptation, the rabbits were carefully anesthetized with 3% pentobarbital sodium (1 ml/kg). The pupils were dilated with 1% tropicamide. The body temperature was maintained at 37 °C with a heating pad to prevent hypothermia. Active gold electrodes were placed onto cornea serving as the recording electrodes. The reference and ground

electrodes were placed subcutaneously in the mid-frontal areas of the head and back, respectively. We performed light stimulation at densities of −2.5, −0.5, −0.02, and 0.5 log (cd*s/m2) for New Zealand white rabbits and 0.5 log (cd*s/m2) for rabbits. The amplitudes and peak times of the a-waves and b-waves were recorded and processed through a RETI-Port device (Roland Consult). All experimental procedures were performed in a dark room under dim red safety light.

Microscopy, Image Acquisition, And Processing

All confocal images were collected by a Zeiss LSM880. Immunostaining data were all processed in ImageJ and Illustrator (Adobe).

Statistical Analysis

Data are shown as the means ± S.D. All statistical tests were performed by PRISM (GraphPad). Statistical significance was detected by Student's t test (parametric). A *P*-value <0.05 was considered statistically significant.

RESULTS

Synthesis of the Poly(acrylamide-co-sodium acrylate) Hydrogel

The new responsive poly(acrylamide-co-sodium acrylate) hydrogel was made from our modified formula as described in the materials and methods section. To produce patterned morphology and structure, a precise 3D-printed IOL mold was injected into the new responsive poly(acrylamide-co-sodium acrylate) hydrogel (Figure 1A). To better adapt for implantation into rabbit eyes, a thin film-like poly(acrylamide-co-sodium acrylate) hydrogel was made (Figure 1B). As a fresh hydrogel often remains unstable and releases small molecular chemical compounds such as glucose, to achieve a stable state of the poly(acrylamide-co-sodium acrylate) hydrogel, we pretreated the hydrogel with PBS and examined its optimal condition to reduce the influence on LECs. We found that after 9 days of pretreatment with PBS, the poly(acrylamide-co-sodium acrylate) hydrogel did not affect the survival or proliferation of LECs (Figure 1C, D).

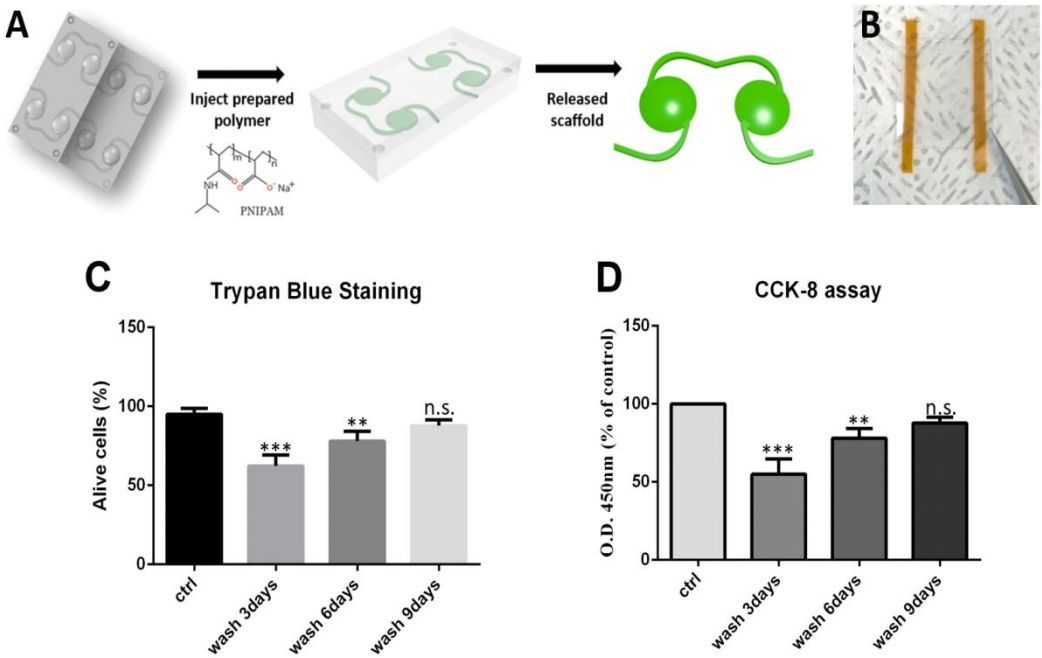

Figure 1 Synthesis of the poly(acrylamide-co-sodium acrylate) hydrogel thin film

A: A precise 3D-printed IOL mold was injected into the new responsive poly(acrylamide-co-sodium acrylate) hydrogel to produce a patterned morphology and structure; B: Image of the poly(acrylamide-co-sodium acrylate) hydrogel thin film; C: Trypan blue staining of LECs co-cocultured with the poly(acrylamide-co-sodium acrylate) hydrogel at 0, 3, 6, and 9 days of the PBS wash; D: CCK8 assay of LECs co-cocultured with the poly(acrylamide-co-sodium acrylate) hydrogel at 0, 3, 6, and 9 days of the PBS wash; Data are shown as the mean±s.d. Independent sample t test. *p < 0.05, **p < 0.01; ***p < 0.005

Effect of the Poly(Acrylamide-Co-Sodium Acrylate) Hydrogel on LECs and ARPE19 Cells *in Vitro*

To investigate whether the poly(acrylamide-co-sodium acrylate) hydrogel disturbs cell viability, we cocultured the poly(acrylamide-co-sodium acrylate) hydrogel with LECs and ARPE19 cells. The cultured cells positively expressed LEC markers, such as PAX6 and SOX2, and synthesized the specific α-A crystallin and negatively expressed the fibroblast cell marker α-SMA, which identified the LECs (Figure 2A~F). When LECs were cocultured with the poly(acrylamide-co-sodium acrylate) hydrogel, cell apoptosis emerged only at the adjacent area around the hydrogel (Figure 2G, H). A similar result could be obtained when it cocultured with ARPE19 cells.

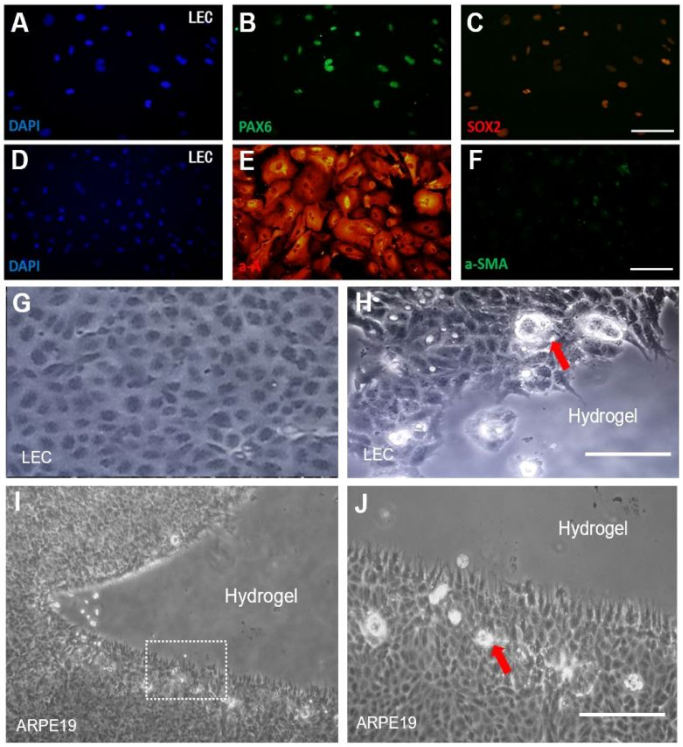

Figure 2 Coculture of poly(acrylamide-co-sodium acrylate) hydrogel thin films with LECs or ARPE19 cells

A~F: Immunostaining of LECs showed that LECs were positively stained for the lens epithelial cell markers PAX6 (A, B), SOX2 (C), and α-A crystallin (D, E) and negatively stained for the fibroblast cell marker α-SMA (F); D~H: Bright field images of LECs co-cultured with (H) or without (G) the poly(acrylamide-co-sodium acrylate) hydrogel. Cells adjacent to the hydrogel were unable to attach to the matrix and ultimately underwent apoptosis (red arrow); I~J: Bright field images of ARPE19 cells co-cultured with the poly(acrylamide-co-sodium acrylate) hydrogel (I). The magnified image (J, white dashed area in I) shows that a minority of adjacent cells

underwent cell apoptosis (red arrow), whereas the distal cells stayed in a normal proliferative state. Scale bar, 50 μm (A~F), 100 μm (G~J).

Implantation of Poly(Acrylamide-Co-Sodium Acrylate) Hydrogel into The Anterior Chamber of New Zealand White Rabbits Does Not Induce Endophthalmitis

To further evaluate the biosafety of poly(acrylamide-co-sodium acrylate) hydrogels, we performed intraocular implantation in New Zealand white rabbits. Slit-lamp imaging at 1 week post-operation indicated corrected location of the hydrogel at the anterior chamber (Figure 3A~C). No significant corneal opacification, keratic precipitate, hypopyon, or synechia was observed at 1 month post-operation among all the groups (Figure 3D~F). Moreover, no anatomic abnormalities were observed at 3 months post-operation among all the groups (Figure 3G~I). In addition, the alteration of IOP after hydrogel implantation was not statistically significant (Figure 4A). To further investigate the effect of poly(acrylamide-co-sodium acrylate) hydrogel implantation on the intraocular inflammatory reaction, we performed ELISA to examine the key inflammatory factors IL-8 and TNF-α. ELISA of the aqueous humor showed that IL-8 (Figure 4B) and TNA-α (Figure 4C) of both the hydrogel and IOL groups were elevated at the first week post-operation, but that of the hydrogel group stayed consistent with that of the control group at 1 month and 3 months post-operation. In sum, implantation of the poly(acrylamide-co-sodium acrylate) hydrogel did not induce any endophthalmitis in the New Zealand white rabbit eyes.

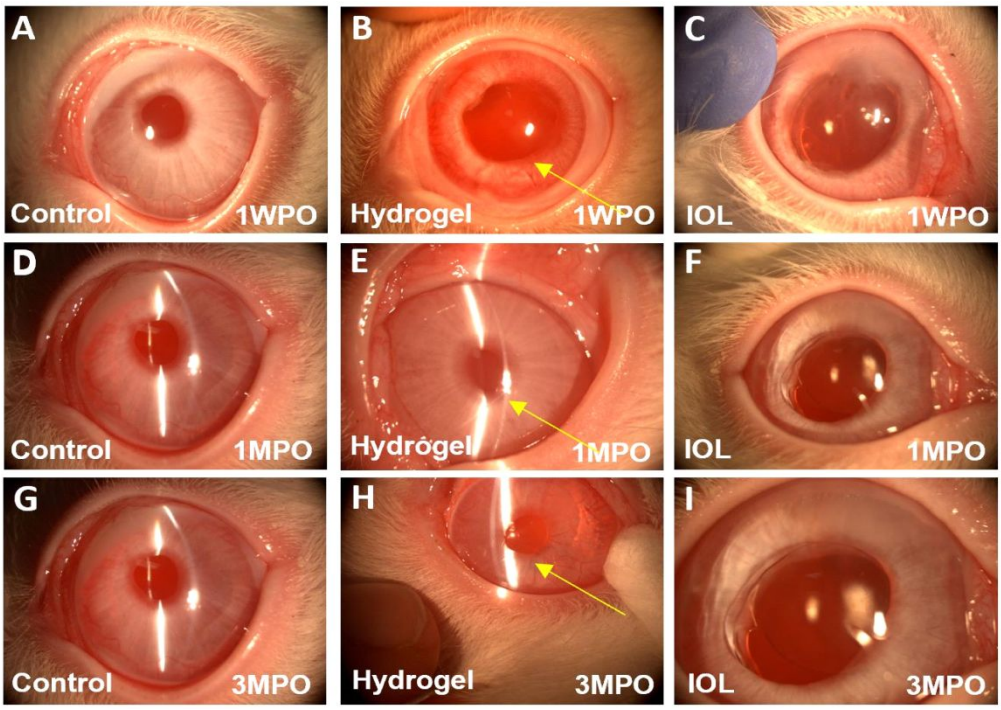

Figure 3 Implantation of poly(acrylamide-co-sodium acrylate) hydrogel thin film into the anterior chamber of New Zealand white rabbits does not induce endophthalmitis

A~C: Slit lamp images of the control group (A), hydrogel group (B) and IOL group (C) at 1 week post-operation showed successful implantation and correct location of the implants; D~F: Slit lamp images of the control group (D), hydrogel group (E) and IOL group (F) at 1 month post-operation showed no significant corneal opacification, keratic precipitate or endophthalmitis; G~I: Slit lamp images of the control group (G), hydrogel group (H) and IOL

group (I) at 3 months post-operation showed no significant corneal opacification, keratic precipitate or endophthalmitis. Week post-operation (WPO); Month post-operation (MPO); Yellow arrow: Hydrogel.

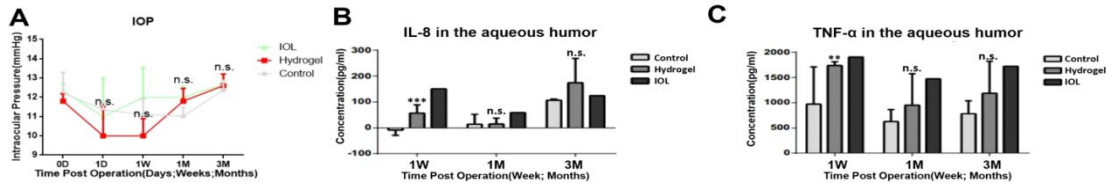

Figure 4 Effects of poly(acrylamide-co-sodium acrylate) hydrogel implantation on the IOP and inflammatory factors in the aqueous humor

A: The IOP recordings revealed showed no significant differences among the control, hydrogel and IOL groups; B~C: ELISA of inflammatory factors such as IL-8 (B) and TNF-α (C) in the aqueous humor of the control, hydrogel and IOL groups; Data are shown as the mean±s.d. Independent sample t test. *$p < 0.05$, **$p < 0.01$; ***$p < 0.005$; n.s. no significance.

Implantation of Poly(Acrylamide-Co-Sodium Acrylate) Hydrogel Does Not Impair Visual Function

Visual function may be well reflected by visual electrophysiology examinations, such as electroretinography (ERG). To further investigate the effect of poly(acrylamide-co-sodium acrylate) hydrogel implantation on visual function, we conducted flash-ERG examinations of the control, hydrogel, and IOL groups. The amplitude of the a-wave of rod, cone and combined rod-cone (Max) ERG 3 months after hydrogel implantation was not significantly altered, nor was the peak time of the wave (Figure 5A, B). Similarly, both the amplitude and peak time of the b-wave of rod, cone and combined rod-cone (Max) ERG 3 months after hydrogel implantation were also not significantly altered (Figure 5C, D). These results indicated normal function of photoreceptor cells and bipolar cells in the hydrogel groups 3 months post-operation. Moreover, we analyzed the characteristics of the Ops wave and light-adapted 30 Hz flicker. Consistent with the results above, the implantation of hydrogel did not affect the amplitude of the Ops wave and light-adapted 30 Hz flicker, as well as its peak time (Figure 5E~G), indicating an intact and well-functioning inner retina and cone system.

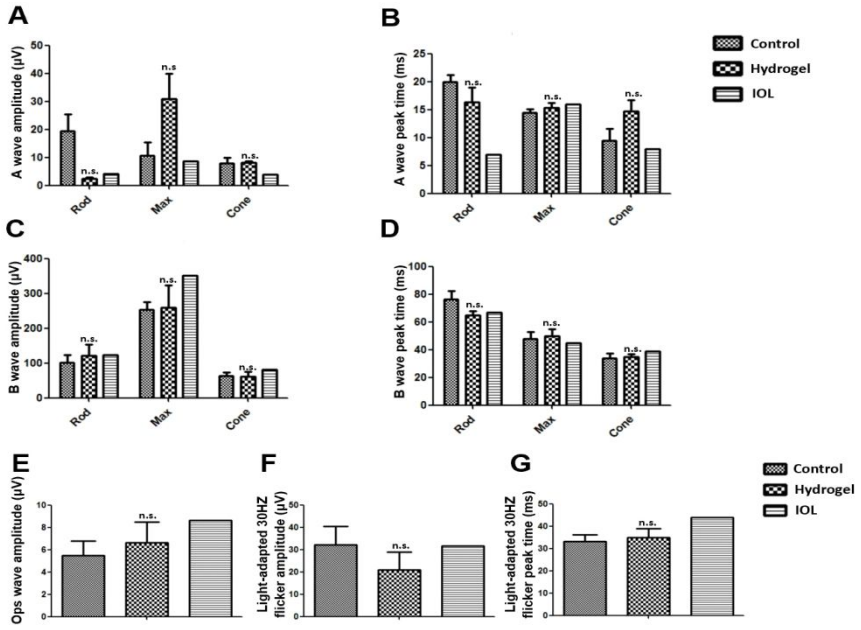

Figure 5 Flash-ERGs of New Zealand white rabbits at 3 months post-implantation

A~B: Statistical analysis of the amplitudes (A) and peak time (B) of fERG a-waves at 0.5 log(cd*s/m^2) in the three groups at 3 months post-operation; C~D: Statistical analysis of the amplitudes (C) and peak time (D) of fERG b-waves at 0.5 log(cd*s/m^2) in the three groups at 3 months post-operation; E~G: Statistical analysis of the Ops wave amplitude (E) at 3.0 log (cd*s/m^2) in the three groups at 3 months post-operation; F~G: Statistical analysis of the light-adapted 30 Hz flicker amplitude (F) and peak time (G) at 3.0 log(cd*s/m^2) in the three groups at 3 months post-operation; Data are shown as the mean±s.d. Independent sample t test. *$p < 0.05$, **$p < 0.01$; ***$p < 0.005$; n.s. no significance.

Implantation of Poly(Acrylamide-Co-Sodium Acrylate) Hydrogel Does Not Damage Ocular Histology

Novel biomaterials are often toxic to the ocular tissue and cause severe abnormalities in histology. To evaluate the effect of poly(acrylamide-co-sodium acrylate) hydrogel implantation on the ocular histology, we first performed HE staining of New Zealand White Rabbit eyes after 3 months of surgery. This result indicated that the hydrogel group maintained its normal histological characteristics, such as cell connections and layered lamination, as well as did the IOL group, all compared with the control group (Figure 6A, B, C). The TUNEL assay revealed that no cellular apoptosis emerged at the cornea, anterior chamber angle (ACA), or retina in any of the three groups, confirming the nontoxic character of the poly(acrylamide-co-sodium acrylate) hydrogel (Figure 7J~R). Moreover, IBA1$^+$ macrophage cells did not accumulate in the cornea or retina except for the ACA in the hydrogel and IOL groups 3 months post-implantation (Figure 7A~I). The recruitment of macrophages at the ACA may represent the immune response caused by the hydrogel or IOL implants, which triggered the phagocytic activation of macrophages.

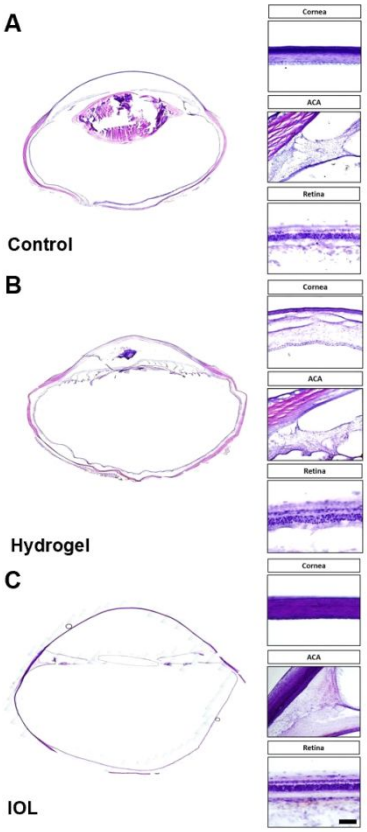

Figure 6 The poly(acrylamide-co-sodium acrylate) hydrogel does not cause histological alteration 3 months post-implantation

A: HE staining of New Zealand White Rabbit eyes showed the detailed histological identity of the cornea, anterior chamber angle, and retina in the control group; B: HE staining of New Zealand White Rabbit eyes showed the detailed histological identity of the cornea, anterior chamber angle, and retina in the hydrogel group. The cell connectivity and layered lamination were normal compared with those of the control group, even though the cornea was ruptured due to the limitations of the HE staining procedure; C: HE staining of New Zealand White Rabbit eyes showed the detailed histological identity of the cornea, anterior chamber angle, and retina in the IOL group. Scale bar, 100 μm.

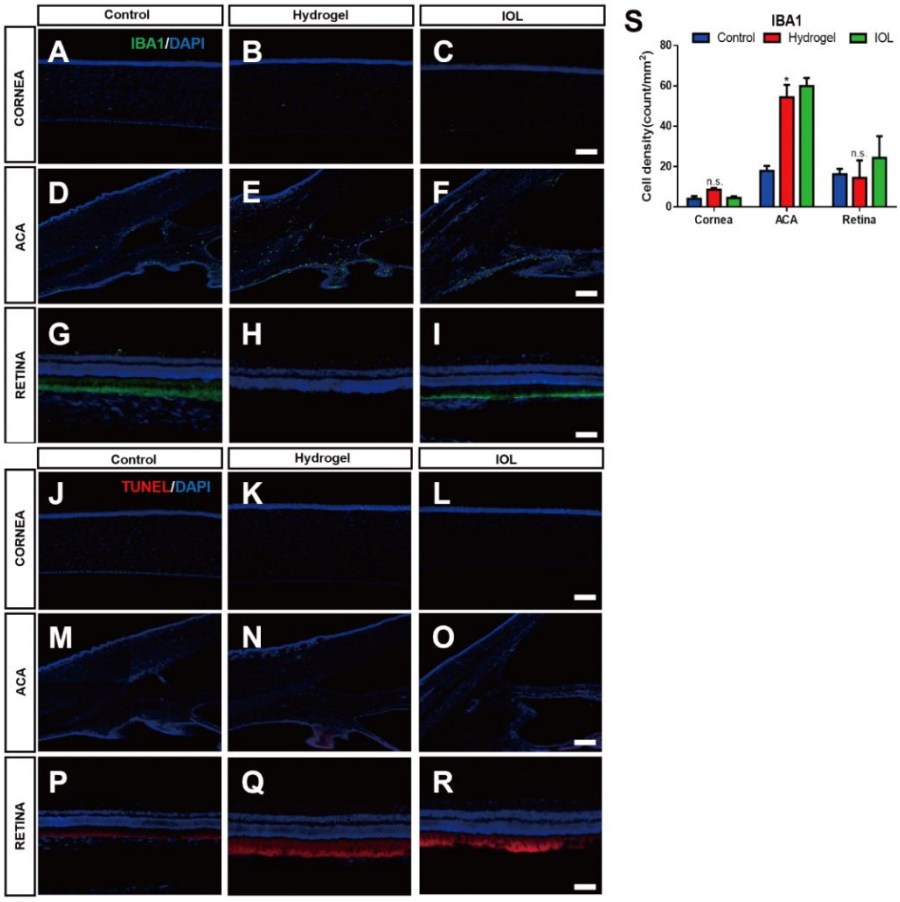

Figure 7 Macrophage activation and cell apoptosis of New Zealand white rabbit eyes 3 months after poly(acrylamide-co-sodium acrylate) hydrogel implantation

A~I: Immunostaining of Iba1 in New Zealand white rabbit eyes at 3 months post-implantation showed Iba1+ macrophage augmentation at the cornea (A~C), ACA (D~F) and retina (G~I) in the control group (A, D, G), the hydrogel group (G, E, H), and the IOL group (C,F,I); J~R: TUNEL assay of New Zealand White Rabbit eyes at 3 months post-implantation showed TUNEL+ apoptotic cell accumulation at the cornea (J~L), ACA (M~O) and retina (P~R) in the control group (J, M, P), the hydrogel group (K, N, Q), and the IOL group (L, O, R); S: Statistical analysis of Iba+ macrophages in the cornea, ANA, and retina in all three groups. Scale bar, 100 μm. Data are shown as the mean±s.d. Independent sample t test. *$p < 0.05$, **$p < 0.01$; ***$p < 0.005$; n.s. no significance.

DISCUSSION

The eye exerts a unique ocular morphology, and all ocular organic architectures are susceptible to a number of diseases that may require treatment via different modalities, such as sustained drug delivery and artificial biotissue substitution.[18] In the past century, hydrogels have been used in various applications as effective materials. The unique network structure of a hydrogel makes it highly hydrophilic and biocompatible, and it exhibits soft physical properties similarly to living tissue, which makes it an ideal and potential biomaterial for ophthalmic applications such as intraocular pumps, injections and implants, reducing comorbidities caused by glaucoma, cataracts, and diabetic retinopathies.[19] 3D printing allows the creation of objects with complex three-dimensional geometries and photologies from a computer-aided design and printed biomaterials to tissue analog structures without any change in their mechanical or biological

properties.[20,21] However, given the nature of the polymers in hydrogel formulations and the materials used in the preparation of ophthalmic gels, it is paramount that any new hydrogel formulation intended for ocular application should be inevitably investigated for potential toxicity/adverse effects on ocular tissues. In this report, we generated a poly(acrylamide-co-sodium acrylate) hydrogel as a thin film and found that the newly formed hydrogel needs 9 days of pretreatment with PBS to stabilize its structure, reflecting the stimuli-controlled phase transition and small molecule release characteristics of stimulus-responsive hydrogels[22]. Second, we performed coculture experiments *in vitro* and implantation experiments *in vivo* to assess the effect of the hydrogel on ocular tissue. The biosafety research parameters for structure, function, and inflammation, such as cell proliferation assays, inflammation detection by slit lamp and aqueous humor tests, visual function assay by electroretinogram, and anatomical abnormality detection by HE staining and immunostaining, all indicated that the poly(acrylamide-co-sodium acrylate) hydrogel is qualified as a biosafe clinical-grade biomaterial for 3D-printed IOLs by systematic investigation and verification both *in vivo* and *in vitro*.

The polymers in preformed ophthalmic hydrogels could be semisynthetic or natural. Some of them can transit from sol to gel conversely triggered by environmental stimuli such as temperature, pH and ion concentration[11,23]. As the poly(acrylamide-co-sodium acrylate) hydrogel was primarily performed by 3D printing, it was harmful to cell proliferation when co-cultured with LECs. (Figure 1C, D). However, pretreatment of the poly(acrylamide-co-sodium acrylate) hydrogel with PBS for 9 days robustly reduced the toxic effect to LECS. This result indicated two points of view: first, the primary poly(acrylamide-co-sodium acrylate) hydrogel could respond to the cell culture environment conditions and release polymers that inhibit cellular proliferation at a high concentration; second, adaptation to the extracellular environment is needed and should be properly investigated and standardized for the safe clinical use of poly(acrylamide-co-sodium acrylate) hydrogels.

When co-cultured with the poly(acrylamide-co-sodium acrylate) hydrogel, both LECs and ARPE19 cells exhibit contact cell death, while cells located far away from the hydrogel grow without any abnormalities. Cell migration and proliferation are highly dependent on the extracellular matrix[24]. To serve as an ideal environment and matrix, ophthalmic hydrogels must be composed of gelatin[25], alginate[26], collagen[27], fibrin[28], and even molecularly modified biomaterials. 3D-printed IOLs have a high light transparency but may be populated by migratory and proliferative cells[29,30]. The contact cell death of the poly(acrylamide-co-sodium acrylate) hydrogel prevented this possibility of this adverse effect of cell migration and proliferation, which makes it an ideal transparent biomaterial with the least opacity after IOL implantation.

A previous study on the ocular tolerability of a new biomaterial formulation used the “Draize rabbit eye irritation test,” which is the oldest and most classic test that has been employed to evaluate potential ocular irritation. However, the Draize test is quite limited by its subjectivity, poor reproducibility and the need for large numbers of live rabbits[31,32]. In the current research, we utilized ELISA to explore the inflammatory factor level of the aqueous humor, and we conducted electroretinogram analyses to examine the visual function after hydrogel implantation. These analyses well addressed the shortcomings of the Draize test and provided distinguished data to gain insight into the effect on ocular inflammation and visual function.

Macrophages are a type of immune cell that engulfs and digests debris, foreign substances, and

microbes [33]. They are patrol guards in the microenvironment of all tissues, which are transformed into active phagocytes by morphology and function and react quickly to various kinds of tissue damage. There is conclusive evidence in animal models and in situ analysis of human tissues that the macrophage response is a common feature of various retinal inflammatory diseases[34-38]. We found accumulated Iba^+ macrophages in the anterior chamber angle and iris of both hydrogel groups 3 months post-operation. The morphology of Iba^+ macrophages in the anterior chamber angle and iris is ameboid like, suggesting that the phagocytic amoeboid movement of emerging macrophages is triggered by hydrogel implantation. Most importantly, we found similar results in the IOL group, which served as a positive biosafe control group, and no corneal opacity, keratic precipitate, hypopyon, or synechia were observed in the hydrogel or IOL group.

As the implanted IOL will be left in the eye for several years after surgery, there is growing interest in the use of IOLs as drug reservoirs or as treatment methods for ophthalmic diseases. Combining 3D printing technology and the biocompatible poly(acrylamide-co-sodium acrylate) hydrogel as the printing material, as well as a potential material for stimuli-responsive hydrogel fabrication, we hold the possibility of loading antibiotics, corticosteroids, and NSAIDs in the IOL, which integrates cataract surgery and postoperative treatments as a one-step procedure[39]. Moreover, IOLs can also be incorporated with telescopic lenses, presbyopia-correcting lenses, or accommodative polyfocal bioanalogical lenses [40,41]. These advanced designs could become more effective and personalized when combined with 3D printing and biocompatible hydrogels. However, all these IOLs inevitably require rigid biosafety assessments and more clinical studies to ascertain their safety and effectiveness.

In sum, the implantation of the poly(acrylamide-co-sodium acrylate) hydrogel did not disturb the IOP, blood parameters, electroretinogram or optical structure, indicating that it will not cause any ocular irritation. However, it is not clear whether this hydrogel lens maintains the nano smooth surface, which can hopefully to correct visual errors, including the defocusing and astigmatism caused by traditional IOLs. We will improve the manufacturing process in the future and test the correction capacity of this new lens in terms of visual quality. Our research provides insight into the biosafety of poly(acrylamide-co-sodium acrylate) hydrogels in ocular tissue and demonstrates that poly(acrylamide-co-sodium acrylate) hydrogels are a safe material for 3D printing of personal IOLs, which hold great potential for future clinical applications.

ACKNOWLEDGMENTS:

Many thanks are due to Doctor Ansu Sun, Mechanical and Construction Engineering, Northumbria University, for their help and support in the preparation and design of poly(acrylamide-co-sodium acrylate) hydrogels.

Author's Contributions:

Jiawen Li: Conception and design, collection and assembly of data, data analysis and interpretation, manuscript writing.

Yijian Li: Collection and assembly of data, data analysis and interpretation

Xisu Hu: Collection and assembly of data

Yu Gong: Collection and assembly of data, data analysis and interpretation

Ben Bin Xu: Design and collection mould of 3D IOL

Haiwei Xu: Critical reading and revision, administrative support, financial support.

Zheng Qin Yin: Financial support, final approval of the manuscript, critical reading and revision.

Foundation:
This study was supported by funding from the Military Medical Science and Technology Innovation Plan (SWH2016LHYS-07), Cultivation Plan of Military Medical Youth Sci-tech (18QNP001).

Conflicts of Interest:
Jiawen Li, None; **Yijian Li**, None; **Xisu Hu**, None; **Yu Gong**, None; **Ben Bin Xu**, None; **Haiwei Xu**, None; **Zheng Qin Yin**, None.

REFERENCES:

1 Liu, Y. C., Wilkins, M., Kim, T., Malyugin, B. & Mehta, J. S. Cataracts. *Lancet* **390**, 600-612, doi:10.1016/s0140-6736(17)30544-5 (2017).
2 Allen, D. & Vasavada, A. Cataract and surgery for cataract. *BMJ (Clinical research ed.)* **333**, 128-132, doi:10.1136/bmj.333.7559.128.
3 Kim, T. I., Alió Del Barrio, J. L., Wilkins, M., Cochener, B. & Ang, M. Refractive surgery. *Lancet (London, England)* **393**, 2085-2098, doi:10.1016/s0140-6736(18)33209-4.
4 Zopf, D. A., Hollister, S. J., Nelson, M. E., Ohye, R. G. & Green, G. E. Bioresorbable airway splint created with a three-dimensional printer. *N. Engl. J. Med.* **368**, 2043-2045, doi:10.1056/NEJMc1206319 (2013).
5 Atala, A., Bauer, S. B., Soker, S., Yoo, J. J. & Retik, A. B. Tissue-engineered autologous bladders for patients needing cystoplasty. *Lancet (London, England)* **367**, 1241-1246, doi:10.1016/s0140-6736(06)68438-9 (2006).
6 Isaacson, A., Swioklo, S. & Connon, C. J. 3D bioprinting of a corneal stroma equivalent. *Exp. Eye Res.* **173**, 188-193, doi:10.1016/j.exer.2018.05.010 (2018).
7 Sommer, A. C. & Blumenthal, E. Z. Implementations of 3D printing in ophthalmology. *Graefe's archive for clinical and experimental ophthalmology = Albrecht von Graefes Archiv fur klinische und experimentelle Ophthalmologie* **257**, 1815-1822, doi:10.1007/s00417-019-04312-3 (2019).
8 Sommer, A. C. & Blumenthal, E. Z. Implementations of 3D printing in ophthalmology. *Graefes Arch. Clin. Exp. Ophthalmol.* **257**, 1815-1822, doi:10.1007/s00417-019-04312-3 (2019).
9 Debellemaniere, G., Flores, M., Montard, M., Delbosc, B. & Saleh, M. Three-dimensional Printing of Optical Lenses and Ophthalmic Surgery: Challenges and Perspectives. *Journal of refractive surgery (Thorofare, N.J. : 1995)* **32**, 201-204, doi:10.3928/1081597x-20160121-05 (2016).
10 Shiblee, M. N. I., Ahmed, K., Khosla, A., Kawakami, M. & Furukawa, H. 3D printing of shape memory hydrogels with tunable mechanical properties. *Soft matter* **14**, 7809-7817, doi:10.1039/c8sm01156g (2018).
11 Al-Kinani, A. A. *et al.* Ophthalmic gels: Past, present and future. *Advanced drug delivery reviews* **126**, 113-126, doi:10.1016/j.addr.2017.12.017 (2018).
12 Hinze, U. *et al.* Implant Design by Means of Multiphoton Polymerization. *Klinische Monatsblatter fur Augenheilkunde* **232**, 1381-1385, doi:10.1055/s-0041-107883 (2015).
13 Chen, X. *et al.* Grafted c-kit+/SSEA1- eye-wall progenitor cells delay retinal degeneration in mice by regulating neural plasticity and forming new graft-to-host synapses. *Stem cell research & therapy* **7**, 191, doi:10.1186/s13287-016-0451-8 (2016).
14 Ullrich M, Aßmus B, Augustin AM, *et al*. SPRED2 deficiency elicits cardiac arrhythmias

and premature death via impaired autophagy. *J. Mol. Cell. Cardiol* **129**:13-26, doi: 10.1016/j.yjmcc.2019.01.023 (2019).
15 Lyu X, Ma Y, Wu F, *et al*. LncRNA NKILA Inhibits Retinoblastoma by Downregulating lncRNA XIST. *Curr. Eye Res* **44**(9):975-979, doi: 10.1080/02713683.2019.1606253 (2019).
16 Yu X, Shen N, Zhang ML, *et al*. Egr-1 decreases adipocyte insulin sensitivity by tilting PI3K/Akt and MAPK signal balance in mice. *Embo j*. **30**(18):3754-65, doi: 10.1038/emboj.2011.277 (2011).
17 Liu W, Liu M, Liu Y, *et al*. Validation and Safety of Visual Restoration by Ectopic Expression of Human Melanopsin in Retinal Ganglion Cells. *Hum. Gene Ther*. **30**(6):714-726. doi: 10.1089/hum.2018.009 (2019).
18 Patel, A., Cholkar, K., Agrahari, V. & Mitra, A. K. Ocular drug delivery systems: An overview. *World journal of pharmacology* **2**, 47-64, doi:10.5497/wjp.v2.i2.47 (2013).
19 Koetting, M. C., Peters, J. T., Steichen, S. D. & Peppas, N. A. Stimulus-responsive hydrogels: Theory, modern advances, and applications. *Materials science & engineering. R, Reports : a review journal* **93**, 1-49, doi:10.1016/j.mser.2015.04.001 (2015).
20 Norman, J., Madurawe, R. D., Moore, C. M., Khan, M. A. & Khairuzzaman, A. A new chapter in pharmaceutical manufacturing: 3D-printed drug products. *Advanced drug delivery reviews* **108**, 39-50, doi:10.1016/j.addr.2016.03.001 (2017).
21 Huang, W. & Zhang, X. 3D Printing: Print the future of ophthalmology. *Investigative ophthalmology & visual science* **55**, 5380-5381, doi:10.1167/iovs.14-15231 (2014).
22 Willner, I. Stimuli-Controlled Hydrogels and Their Applications. *Accounts of chemical research* **50**, 657-658, doi:10.1021/acs.accounts.7b00142 (2017).
23 Craig, J. P., Singh, I., Tomlinson, A., Morgan, P. B. & Efron, N. The role of tear physiology in ocular surface temperature. *Eye* **14 (Pt 4)**, 635-641, doi:10.1038/eye.2000.156 (2000).
24 Cope, E. C. & Gould, E. Adult Neurogenesis, Glia, and the Extracellular Matrix. *Cell stem cell* **24**, 690-705, doi:10.1016/j.stem.2019.03.023 (2019).
25 Billiet, T., Gevaert, E., De Schryver, T., Cornelissen, M. & Dubruel, P. The 3D printing of gelatin methacrylamide cell-laden tissue-engineered constructs with high cell viability. *Biomaterials* **35**, 49-62, doi:10.1016/j.biomaterials.2013.09.078 (2014).
26 Duan, B., Hockaday, L. A., Kang, K. H. & Butcher, J. T. 3D bioprinting of heterogeneous aortic valve conduits with alginate/gelatin hydrogels. *Journal of biomedical materials research. Part A* **101**, 1255-1264, doi:10.1002/jbm.a.34420 (2013).
27 Mazzocchi, A., Devarasetty, M., Huntwork, R., Soker, S. & Skardal, A. Optimization of collagen type I-hyaluronan hybrid bioink for 3D bioprinted liver microenvironments. *Biofabrication* **11**, 015003, doi:10.1088/1758-5090/aae543 (2018).
28 Lee, Y. B. *et al.* Bio-printing of collagen and VEGF-releasing fibrin gel scaffolds for neural stem cell culture. *Exp Neurol* **223**, 645-652, doi:10.1016/j.expneurol.2010.02.014 (2010).
29 Buwalda, S. J. & Vermonden, T. Hydrogels for Therapeutic Delivery: Current Developments and Future Directions. **18**, 316-330, doi:10.1021/acs.biomac.6b01604 (2017).
30 Wu, Z. *et al.* Bioprinting three-dimensional cell-laden tissue constructs with controllable degradation. *Scientific reports* **6**, 24474, doi:10.1038/srep24474 (2016).
31 Lordo, R. A., Feder, P. I. & Gettings, S. D. Comparing and evaluating alternative (in vitro) tests on their ability to predict the Draize maximum average score. *Toxicology in vitro : an international journal published in association with BIBRA* **13**, 45-72,

doi:10.1016/s0887-2333(98)00062-9 (1999).
32 Abdelkader, H. *et al.* Conjunctival and corneal tolerability assessment of ocular naltrexone niosomes and their ingredients on the hen's egg chorioallantoic membrane and excised bovine cornea models. *International journal of pharmaceutics* **432**, 1-10, doi:10.1016/j.ijpharm.2012.04.063 (2012).
33 Ovchinnikov, D. A. Macrophages in the embryo and beyond: much more than just giant phagocytes. *Genesis (New York, N.Y. : 2000)* **46**, 447-462, doi:10.1002/dvg.20417 (2008).
34 Karlstetter, M. *et al.* Retinal microglia: just bystander or target for therapy? *Prog Retin Eye Res* **45**, 30-57, doi:10.1016/j.preteyeres.2014.11.004 (2015).
35 Rathnasamy, G., Foulds, W. S., Ling, E. A. & Kaur, C. Retinal microglia - A key player in healthy and diseased retina. *Progress in neurobiology* **173**, 18-40, doi:10.1016/j.pneurobio.2018.05.006 (2019).
36 Kanazawa, H., Ohsawa, K., Sasaki, Y., Kohsaka, S. & Imai, Y. Macrophage/microglia-specific protein Iba1 enhances membrane ruffling and Rac activation via phospholipase C-gamma -dependent pathway. *The Journal of biological chemistry* **277**, 20026-20032, doi:10.1074/jbc.M109218200 (2002).
37 Okayasu, T., Quesnel, A. M., O'Malley, J. T., Kamakura, T. & Nadol, J. B., Jr. The Distribution and Prevalence of Macrophages in the Cochlea Following Cochlear Implantation in the Human: An Immunohistochemical Study Using Anti-Iba1 Antibody. *Otology & neurotology : official publication of the American Otological Society, American Neurotology Society [and] European Academy of Otology and Neurotology*, doi:10.1097/mao.0000000000002495 (2019).
38 Cora, M. C. & Janardhan, K. S. Previously Diagnosed Reticulum Cell Hyperplasia in Decalcified Rat Bone Marrow Stain Positive for Ionized Calcium Binding Adapter Molecule 1 (Iba1): A Monocytic/Macrophage Cell Marker. 192623319890610, doi:10.1177/0192623319890610 (2019).
39 Liu, Y. C., Wong, T. T. & Mehta, J. S. Intraocular lens as a drug delivery reservoir. *Curr Opin Ophthalmol* **24**, 53-59, doi:10.1097/ICU.0b013e32835a93fc (2013).
40 Boyer, D., Freund, K. B., Regillo, C., Levy, M. H. & Garg, S. Long-term (60-month) results for the implantable miniature telescope: efficacy and safety outcomes stratified by age in patients with end-stage age-related macular degeneration. *Clin Ophthalmol* **9**, 1099-1107, doi:10.2147/opth.S86208 (2015).
41 Ford, J., Werner, L. & Mamalis, N. Adjustable intraocular lens power technology. *J Cataract Refract Surg* **40**, 1205-1223, doi:10.1016/j.jcrs.2014.05.005 (2014).

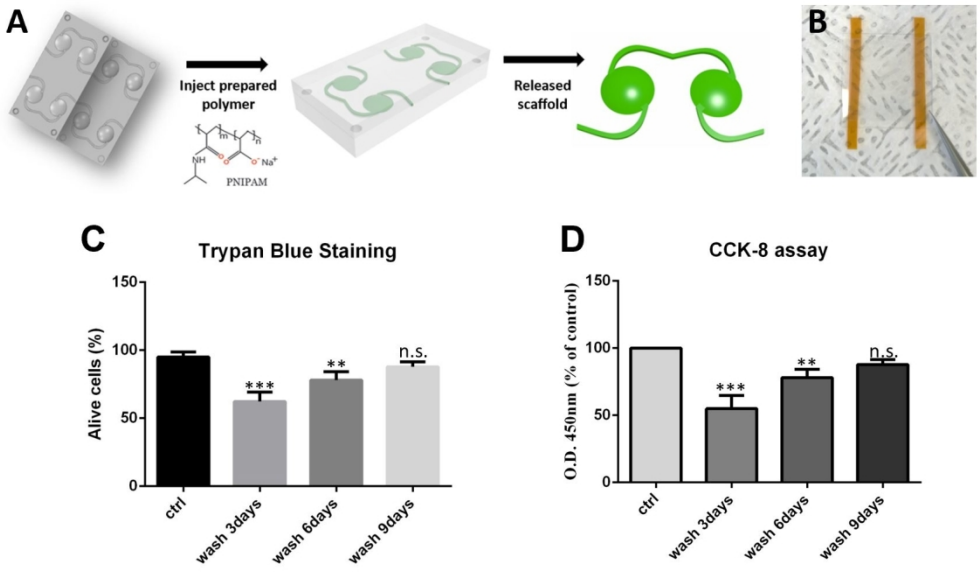

Figure1

202x118mm (216 x 216 DPI)

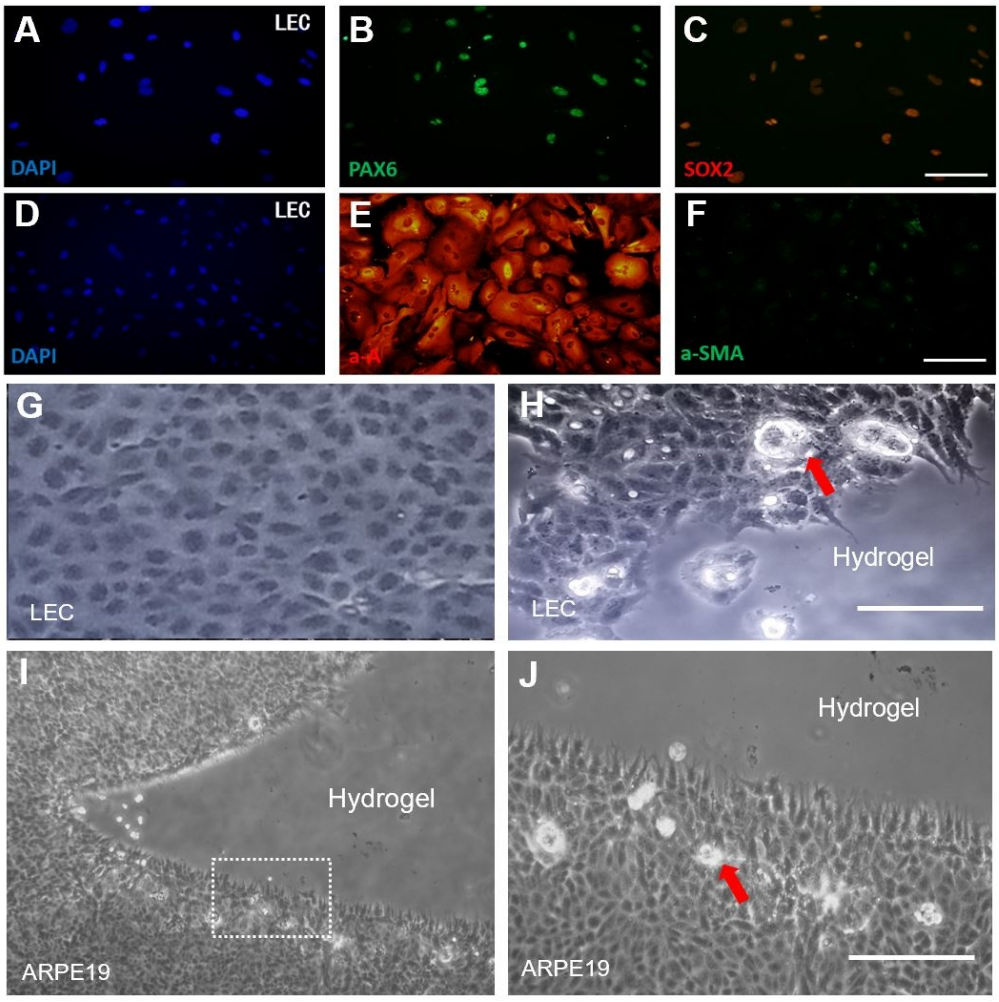

Figure2

123x123mm (216 x 216 DPI)

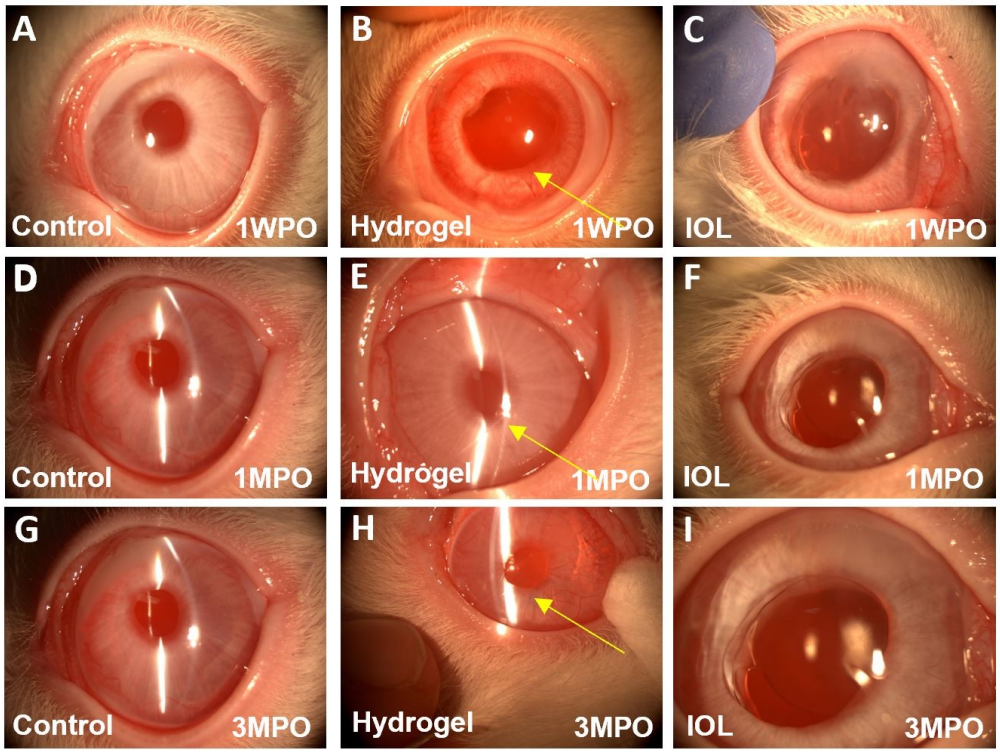

Figure3

155x117mm (216 x 216 DPI)

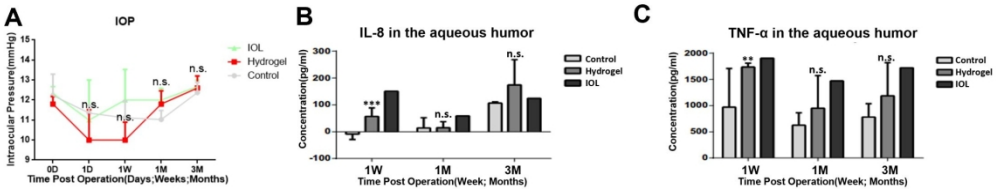

Figure4

259x49mm (216 x 216 DPI)

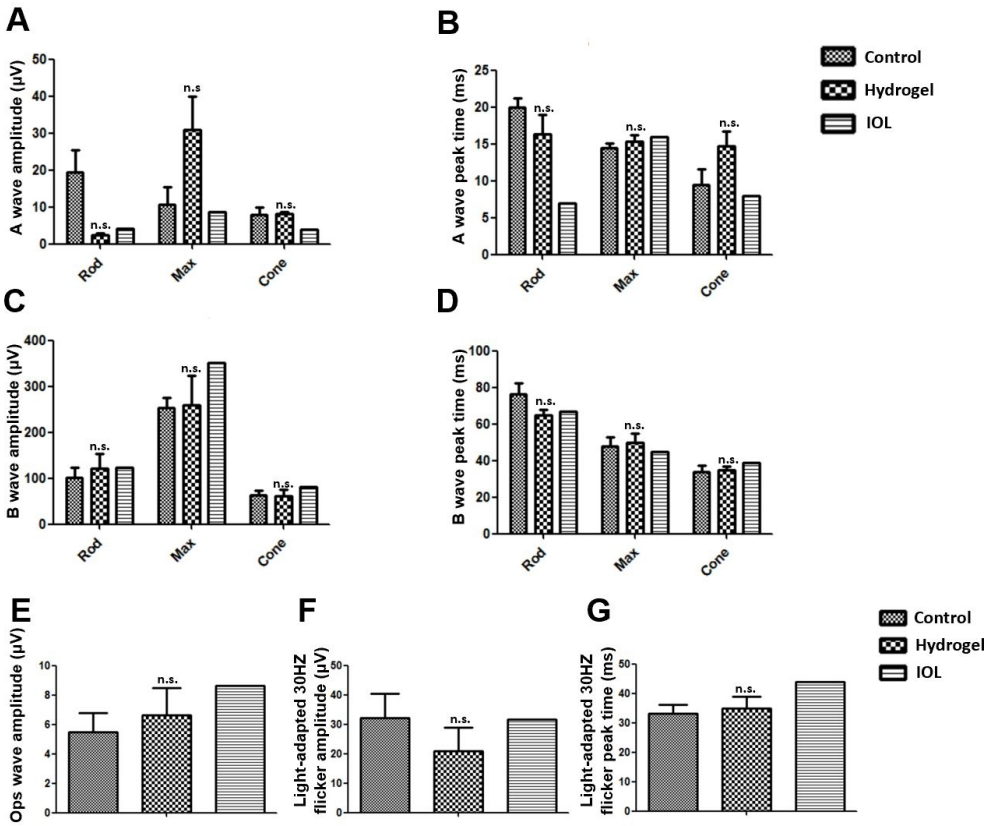

Figure5

150x125mm (216 x 216 DPI)

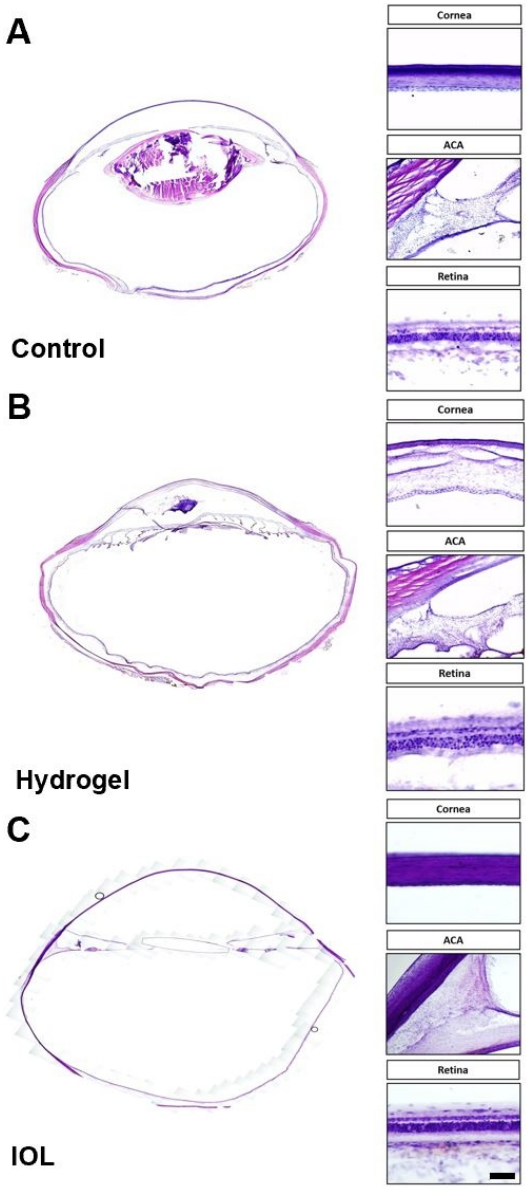

Figure6

59x133mm (216 x 216 DPI)

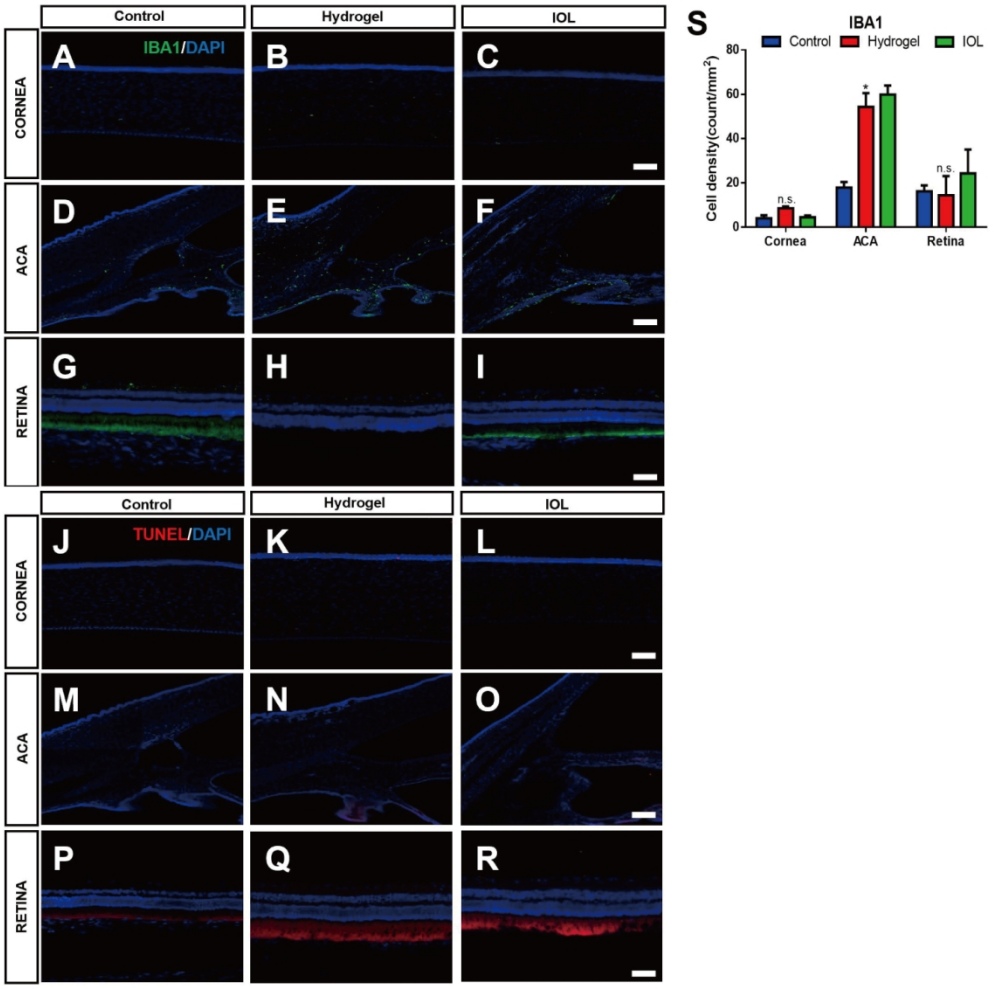
Control
Hydrogel
IOL
CORNEA
ACA
RETINA
A
IBA1/DAPI
B
C
D
E
F
G
H
I
J
TUNEL/DAPI
K
L
M
N
O
P
Q
R
S
IBA1
Control
Hydrogel
IOL
Cell density(count/mm²)
80
60
40
20
0
n.s.
*
n.s.
Cornea
ACA
Retina

Figure7

Biosafety of a 3D-printed Intraocular Lens Made of a Poly(Acrylamide-Co-Sodium Acrylate) Hydrogel *In Vitro* and *In Vivo*

Running title: Biosafety of Poly(Acrylamide-Co-Sodium Acrylate) as IOL material

Jiawen Li,[1,2] Yijian Li,[1,2] Xisu Hu, [1,2] Yu Gong,[1,2] Ben Bin Xu,[3] Haiwei Xu,[1,2] Zheng Qin Yin[1,2]

[1]Southwest Hospital/Southwest Eye Hospital, Third Military Medical University (Army Medical University), Chongqing, P.R. China

[2]Key Lab of Visual Damage and Regeneration & Restoration of Chongqing, Chongqing, P.R. China

[3]Smart Materials and Surfaces Lab, Faculty of Engineering and Environment, Northumbria University, Newcastle upon Tyne NE1 8ST, UK

Correspondence to: Haiwei Xu and Zheng Qin Yin. Southwest Hospital/Southwest Eye Hospital, Third Military Medical University (Army Medical University), Chongqing 400038, P.R. China.

E-mail addresses: xuhaiwei@tmmu.edu.cn; qinzyin@aliyun.com

ACKNOWLEDGMENTS:

Many thanks are due to Doctor Ansu Sun, Mechanical and Construction Engineering, Northumbria University, for their help and support in the preparation and design of poly(acrylamide-co-sodium acrylate) hydrogels.

Author's Contributions:

Jiawen Li: Conception and design, collection and assembly of data, data analysis and interpretation, manuscript writing. Yijian Li: Collection and assembly of data, data analysis and interpretation. Xisu Hu: Collection and assembly of data. Yu Gong: Collection and assembly of data, data analysis and interpretation. Ben Bin Xu: Design and collection mould of 3D IOL. Haiwei Xu: Critical reading and revision, administrative support, financial support. Zheng Qin Yin: Financial support, final approval of the manuscript, critical reading and revision.

Foundation:

This study was supported by funding from the Military Medical Science and Technology Innovation Plan (SWH2016LHYS-07), Cultivation Plan of Military Medical Youth Sci-tech (18QNP001).

Conflicts of Interest:

Jiawen Li, None; **Yijian Li**, None; **Xisu Hu**, None; **Yu Gong**, None; **Ben Bin Xu**, None; **Haiwei Xu**, None; **Zheng Qin Yin**, None.

Abstract

AIM: To assess the biosafety of a poly(acrylamide-co-sodium acrylate) hydrogel as a 3D-printed intraocular lens (IOL) material.

METHODS: The biosafety of the poly(acrylamide-co-sodium acrylate) hydrogel was first analyzed *in vitro* using human lens epithelial cells (LECs) and the ARPE19 cell line, and a CCK-8 assay was performed to investigate alterations in cell proliferation. A thin film of a poly(acrylamide-co-sodium acrylate) hydrogel and a conventional IOL were intraocularly implanted into the eyes of New Zealand white rabbits respectively, and a sham surgery served as control group. The anterior segment photographs, intraocular pressure (IOP), blood parameters and electroretinograms were recorded. Inflammatory cytokines in the aqueous humor, such as TNFα and IL-8, were examined by ELISA. Cell apoptosis of the retina was investigated by TUNEL assay, and macrophage activation was detected by immunostaining.

RESULTS: The poly(acrylamide-co-sodium acrylate) hydrogel did not slow cell proliferation when cocultured with human LECs or ARPE19 cells. The implantation of a thin film of a 3D-printed IOL composed of the poly(acrylamide-co-sodium acrylate) hydrogel did not affect the IOP, blood parameters, electroretinogram or optical structure in any of the three experimental groups (n=3 for each group). Both TNFα and IL-8 in the aqueous humor of the hydrogel group were transiently elevated 1 week post-operation and recovered to normal levels at 1 and 3 months post-operation. $Iba1^+$ macrophages in the anterior chamber angle of the hydrogel group were increased markedly compared to those of the control group; however, there was no significant difference compared to those in the IOL group.

CONCLUSION: The poly(acrylamide-co-sodium acrylate) hydrogel is a safe material for 3D printing of personal IOLs that hold great potential for future clinical applications.

KEYWORDS: Cataract; Biosafety; Lens Epithelial Cells; ARPE19 Cells; Intraocular Lens; 3D Printing; Poly Hydrogel; Rabbit

INTRODUCTION

More than 95 million people worldwide have cataracts, which is the leading cause of blindness.[1] Phacoemulsification combined with intraocular lens (IOL) implantation is the most effective way to treat cataract so far.[2] However, the mass-produced model IOL based on a high-precision machine tool fails to meet the growing demands of personalized customization of the human lens, and it is hard to obtain the best postoperative vision.[3] Precision medicine is an inevitable trend in the development of clinical medicine, personalized customization is an extremely important component of precision medicine, and personalized IOL customization is an important means

to improve the outcome of cataract surgery.

3D printing holds great potential in biomedical engineering research as well as in ophthalmologic applications,[4-6] which enables cost-effective products and instruments that aid in therapeutic devices, such as IOLs, built specifically for individual cataract patients.[7] Based on the clinical data, it is possible for us to design a personalized IOL suitable for the size of the lens capsule by digital optical modeling, simulating the quality of IOL imaging and correcting the wave front aberration.[8] Achievement of 3D printing of IOLs is a great challenge, and the breakthrough bottleneck lies in the following points: 1) the fabrication of ultrahigh-precision roughness of the IOL surface (micro/nano-precision);[9] 2) the high transparency and UV-blocking ability of materials; 3) the flexibility, water richness and micromechanical characteristics of the organic materials; and 4) the biosafety of the material for 3D-printed IOLs.[10,11]

Additive manufacturing and 3D printing create new approaches for the design and manufacturing of implants, such as microstructured eye implants, including multifocal diffractive aspheric IOL.[12] We planned to print the IOL mold with a new responsive poly(acrylamide-co-sodium acrylate) hydrogel with 3D precise printing technology, which aims to provide accurate and personalized IOL products for cataract patients. The gel is a fully diluted crosslinking system that has no fluidity in the stable state. The main component of the gel is liquid by weight. However, due to the 3D crosslinking network, the structural integrity of the hydrogel network will not be dissolved due to the high hydrophilicity. Hydrogels are highly absorbent and light permeable (containing more than 90% water). Due to its high water content, the hydrogel also has a very similar flexibility to natural tissue, which makes it an ideal 3D printing material for making personalized IOLs. However, as responsive smart materials, hydrogels can encapsulate chemical compounds such as glucose, which are released by the stimulation of external factors, such as changes in pH. Thus, whether a poly(acrylamide-co-sodium acrylate) hydrogel is toxic to ocular tissue needs to be deliberately considered. Nevertheless, the issue of the biosafety of poly(acrylamide-co-sodium acrylate) hydrogels is unclear so far.

Here, we utilized a poly(acrylamide-co-sodium acrylate) hydrogel to create a thin film in order to investigate its biosafety after intraocular implantation. It was demonstrated *in vivo* that IOP, ERGs and inflammatory factors in the aqueous humor exhibited no significant difference after poly(acrylamide-co-sodium acrylate) hydrogel implantation. Moreover, similar results could be verified by experiments *in vitro*. Taken together, the results indicate that the poly(acrylamide-co-sodium acrylate) hydrogel does not harm the rabbit ocular tissue and causes no inflammation *in vitro* or *in vivo*, supporting the idea that it is a safe material for on-demand manufacturing of patient-personalized IOLs.

MATERIALS AND METHODS

Laboratory Animal Welfare

All experiments were performed on New Zealand white rabbits provided by the Experimental Animal Centre of Southwest Hospital, Army Medical University. The New Zealand white rabbits were all raised in the Animal Care Centre of the Army Medical University and maintained with free access to water and food under a 12-h light/dark cycle. All animal experimental procedures were formally approved by the Institutional Review Board of the Army Medical University.

Preparation of the Poly(Acrylamide-Co-Sodium Acrylate) Hydrogel Thin Film

The hydrogel solution was prepared according to the following formula: 17.5% N-isopropylacrylamide; 12.5% sodium acrylate; 1.5% N,N'-methylenebisacrylamide; N,N,N',N'-tetramethylethylenediamine; 10% ammonium persulfate, H_20. The solution was added to one of the molds and immediately joined with another mold. Then, the two pieces of mold were clamped together. After 30~60 minutes, after the gel was solidified, and the two molds were removed. The formed hydrogel crystals were transferred to phosphate buffered saline (PBS) for preservation.

Intraocular Implantation of the Poly(Acrylamide-Co-Sodium Acrylate) Hydrogel Thin Film into New Zealand White Rabbit Eyes

The New Zealand white rabbits were divided into three groups based on implants: the poly(acrylamide-co-sodium acrylate) hydrogel thin film as the hydrogel group, the conventional IOL as the IOL group, and the sham surgery as the control group (n=3 for each group). Animals were anesthetized with 3% pentobarbital sodium 1 ml/kg through the ear-rim auricular vein; the left eye was selected as the operative eye. Before the operation, tropicamide eye drops (Santen) were used for mydriasis. The eyelid was opened with an eye speculum, and the conjunctival sac was soaked with 5% povidone iodine for 90 seconds and then rinsed with saline. A 3.0 mm width transparent corneal incision was made at the 12 o'clock position, a 1.0 mm width auxiliary corneal incision was made at the 9 o'clock position, and sodium hyaluronate (SINGCLEAN) was injected into the anterior chamber. For the control group, the incision was sutured directly with 10-0 polypropylene. For the hydrogel group and IOL group, we performed capsulorhexis, water separation, and phacoemulsification of the lens nucleus (Laureate, Alcon, USA), cleared the lens cortex with I/A, and injected the poly(acrylamide-co-sodium acrylate) hydrogel thin film (5 mm×5 mm) or IOL (860 UV, acrylic intraocular lenses as a positive control of biosafety). The 12 o'clock incision was sutured with 10-0 nylon suture, balanced salt solution (BSS) was injected to form the anterior chamber capacity, and tobramycin dexamethasone eye ointment (Alcon, USA) was applied to the eyes after the operation. Intraocular pressures (IOP) was measured by a

noncontact tonometer at 1 day, 1 week, 1 month, and 3 months post-operation.

Euthanasia and Histopathology

Three months after implantation, the New Zealand white rabbits were euthanized with pentobarbital sodium (400 mg/kg) administered intravenously. Afterwards, each eye containing the implant was taken from each rabbit for histological examination. Specimens were fixed in 4% paraformaldehyde for at least 24 hours and dehydrated in 30% sucrose for at least 24 hours, followed by embedding with Tissue-Tek O.C.T. Compound (Sakura Finetek USA, Inc., Torrance, CA 90501, USA). All tissue pieces were cut into 2–4 μm thick tissue sections (Leica CM1900UV cryostat). Then, all sections were routinely stained with hematoxylin-eosin (HE) and examined under a light microscope (OLYMPUS DP71; Olympus Europa SE & Co. KG, Hamburg, Germany) to assess fibroblast proliferation and anatomical abnormalities.

Cell Culture

Human lens epithelial cells (LECs) were expanded from lens explants, which were provided by the Southwest Hospital Eye Bank. Briefly, the lens was washed in cold PBS containing 50 U mL^{-1} penicillin and 100 μg mL^{-1} streptomycin, cut into 5 mm×5 mm small pieces and seeded onto human vitronectin (Gibco, Thermo Fisher, USA) precoated plates, and the explants were left for attachment. The second day, LECs were cultured in conditioned medium consisting of DMEM/F12 (HyClone), 10% FBS (Gibco), insulin-transferrin sodium selenite (1 μg mL^{-1}, Gibco), penicillin (100 U mL^{-1}) and streptomycin (100 μg mL^{-1}, HyClone). As cells reached subconfluence, they were gently passaged at 1:6 to expand. The ARPE19 cell line was cultured according to the same procedures and conditions described above. The cells were co-cultured with the poly(acrylamide-co-sodium acrylate) hydrogel thin film (5 mm×5 mm) or PBS as control.

Immunostaining to Identify LECs

Immunostaining was routinely performed as previously described.[13] Sections were incubated for 15 minutes with PBS, and sections were further incubated with PBS containing 0.1% (vol/vol) Triton X-100 for 15 minutes and further blocked with 1% (wt/vol) bovine serum albumin (BSA) in PBS at room temperature. The following primary antibodies were incubated at 4℃ overnight: Pax6 (1:500, Abcam), Sox2 (1:400, Abcam), αA-crystallin (1:200, Santa Cruz), α-SMA (1:400, Abcam), and Iba1 (1:500, Wako).

TUNEL Staining to Analyze the Apoptotic Cells and Immuno Cells in the Eyes Of Rabbits

Using the TUNEL Assay Kit (Abcam) as previously described[14], the secondary antibodies included the goat anti-mouse Alexa Fluor 488 and goat anti-mouse Alexa Fluor 594 (Invitrogen). DAPI (1:10, Beyotime) was incubated for 8-10 minutes at 20℃ to counterstain nuclei, followed by cover-slipping with antifade mounting medium (Beyotime).

CCK-8 Assay to Analyze the Proliferation of LECs and APRE19 Cells

The cytotoxicity of the poly(acrylamide-co-sodium acrylate) hydrogel was measured using the Cell Counting Kit-8 (CCK-8) assay according to a previously published protocol.[15] Absorbance at wavelengths of 450 and 650 nm was collected using a microplate reader (Varioskan Flash, Thermo Fisher, USA).

ELISA Assay to Analyze Cytokines

The aqueous humor was extracted with a 30G sterile needle syringe at the 9 o'clock position of the limbus at 1 week, 1 month, and 3 months post-operation. ELISAs to detect IL-8 and TNF (cloud-clone corp.) were performed as previously reported.[16] The absorbance of each well was read at 450 nm and 550 nm. The 550 nm values were subtracted from the 450 nm values to correct for optical imperfections in the microplate.

Electroretinogram Recording to Assess The Visual Function of Rabbits

Scotopic flash electroretinogram recording was performed at 3 months post-operation as described previously.[17] Briefly, after 12-h dark adaptation, the rabbits were carefully anesthetized with 3% pentobarbital sodium (1 ml/kg). The pupils were dilated with 1% tropicamide. The body temperature was maintained at 37 °C with a heating pad to prevent hypothermia. Active gold electrodes were placed onto cornea serving as the recording electrodes. The reference and ground electrodes were placed subcutaneously in the mid-frontal areas of the head and back, respectively. We performed light stimulation at densities of −2.5, −0.5, −0.02, and 0.5 log (cd*s/m2) for New Zealand white rabbits and 0.5 log (cd*s/m2) for rabbits. The amplitudes and peak times of the a-waves and b-waves were recorded and processed through a RETI-Port device (Roland Consult). All experimental procedures were performed in a dark room under dim red safety light.

Microscopy, Image Acquisition, And Processing

All confocal images were collected by a Zeiss LSM880. Immunostaining data were all processed in ImageJ and

Illustrator (Adobe).

Statistical Analysis

Data are shown as the means ± S.D. All statistical tests were performed by PRISM (GraphPad). Statistical significance was detected by Student's t test (parametric). A *P*-value <0.05 was considered statistically significant.

RESULTS

Synthesis of the Poly(acrylamide-co-sodium acrylate) Hydrogel

The new responsive poly(acrylamide-co-sodium acrylate) hydrogel was made from our modified formula as described in the materials and methods section. To produce patterned morphology and structure, a precise 3D-printed IOL mold was injected into the new responsive poly(acrylamide-co-sodium acrylate) hydrogel (Figure 1A). To better adapt for implantation into rabbit eyes, a thin film-like poly(acrylamide-co-sodium acrylate) hydrogel was made (Figure 1B). As a fresh hydrogel often remains unstable and releases small molecular chemical compounds such as glucose, to achieve a stable state of the poly(acrylamide-co-sodium acrylate) hydrogel, we pretreated the hydrogel with PBS and examined its optimal condition to reduce the influence on LECs. We found that after 9 days of pretreatment with PBS, the poly(acrylamide-co-sodium acrylate) hydrogel did not affect the survival or proliferation of LECs (Figure 1C, D).

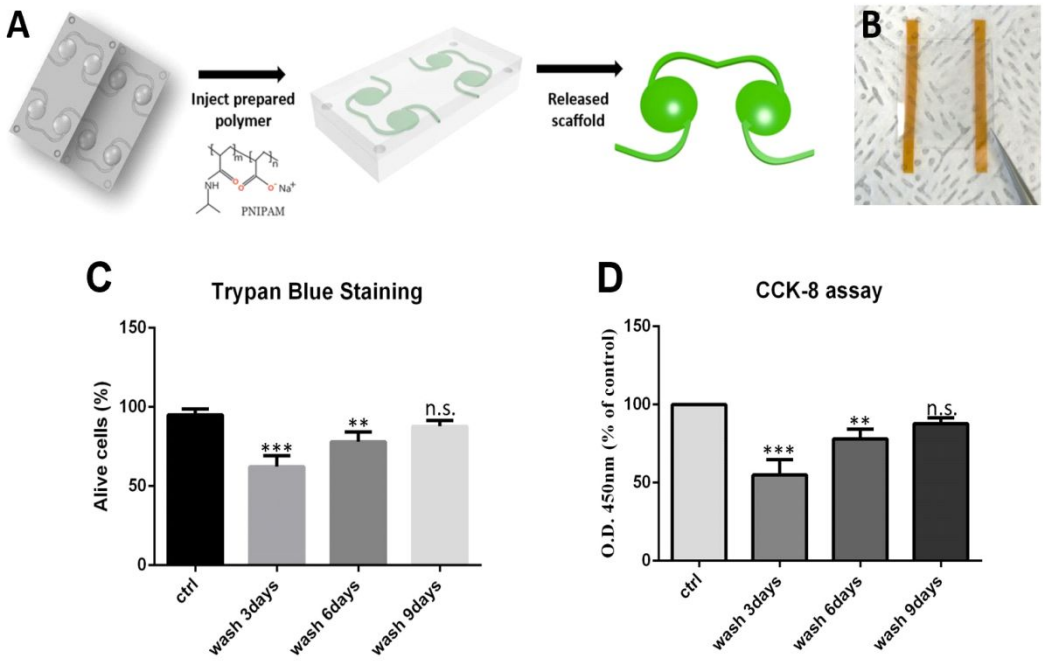

Figure 1 Synthesis of the poly(acrylamide-co-sodium acrylate) hydrogel thin film

A: A precise 3D-printed IOL mold was injected into the new responsive poly(acrylamide-co-sodium acrylate) hydrogel to produce a patterned morphology and structure; B: Image of the poly(acrylamide-co-sodium acrylate) hydrogel thin film; C: Trypan blue staining of LECs co-cocultured with the poly(acrylamide-co-sodium acrylate) hydrogel at 0, 3, 6, and 9 days of the PBS wash; D: CCK8 assay of LECs co-cocultured with the poly(acrylamide-co-sodium acrylate) hydrogel at 0, 3, 6, and 9 days of the PBS wash; Data are shown as the mean±s.d. Independent sample t test. *p < 0.05, **p < 0.01; ***p < 0.005

Effect of the Poly(Acrylamide-Co-Sodium Acrylate) Hydrogel on LECs and ARPE19 Cells *in Vitro*

To investigate whether the poly(acrylamide-co-sodium acrylate) hydrogel disturbs cell viability, we cocultured the poly(acrylamide-co-sodium acrylate) hydrogel with LECs and ARPE19 cells. The cultured cells positively expressed LEC markers, such as PAX6 and SOX2, and synthesized the specific α-A crystallin and negatively expressed the fibroblast cell marker α-SMA, which identified the LECs (Figure 2A~F). When LECs were cocultured with the poly(acrylamide-co-sodium acrylate) hydrogel, cell apoptosis emerged only at the adjacent area around the hydrogel (Figure 2G, H). A similar result could be obtained when it cocultured with ARPE19 cells.

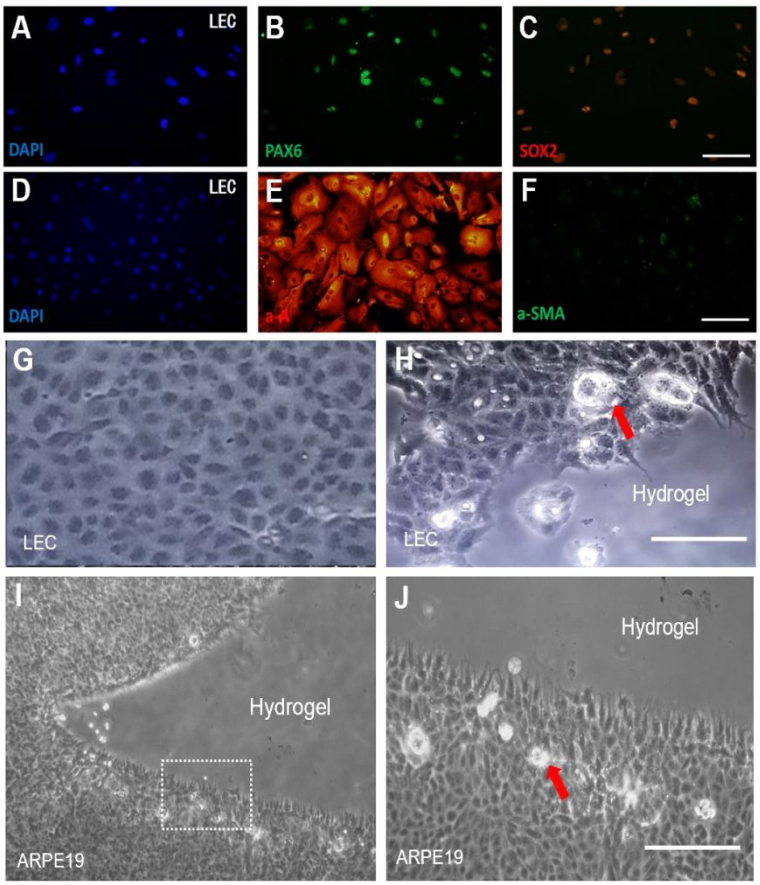

Figure 2 Coculture of poly(acrylamide-co-sodium acrylate) hydrogel thin films with LECs or ARPE19 cells A~F: Immunostaining of LECs showed that LECs were positively stained for the lens epithelial cell markers PAX6 (A, B), SOX2 (C), and α-A crystallin (D, E) and negatively stained for the fibroblast cell marker α-SMA (F); D~H: Bright field images of LECs co-cultured with (H) or without (G) the poly(acrylamide-co-sodium acrylate) hydrogel. Cells adjacent to the hydrogel were unable to attach to the matrix and ultimately underwent apoptosis (red arrow); I~J: Bright field images of ARPE19 cells co-cultured with the poly(acrylamide-co-sodium acrylate) hydrogel (I). The magnified image (J, white dashed area in I) shows that a minority of adjacent cells underwent cell apoptosis (red arrow), whereas the distal cells stayed in a normal proliferative state. Scale bar, 50 μm (A~F), 100 μm (G~J).

Implantation of Poly(Acrylamide-Co-Sodium Acrylate) Hydrogel into The Anterior Chamber of New Zealand White Rabbits Does Not Induce Endophthalmitis

To further evaluate the biosafety of poly(acrylamide-co-sodium acrylate) hydrogels, we performed intraocular implantation in New Zealand white rabbits. Slit-lamp imaging at 1 week post-operation indicated corrected location of the hydrogel at the anterior chamber (Figure 3A~C). No significant corneal opacification, keratic precipitate, hypopyon, or synechia was observed at 1 month post-operation among all the groups (Figure 3D~F). Moreover, no anatomic abnormalities were observed at 3 months post-operation among all the groups (Figure 3G~I). In addition, the alteration of IOP after hydrogel implantation was not statistically significant (Figure 4A). To further investigate the effect of poly(acrylamide-co-sodium acrylate) hydrogel implantation on the intraocular inflammatory reaction, we performed ELISA to examine the key inflammatory factors IL-8 and TNF-α. ELISA of the aqueous humor showed that IL-8 (Figure 4B) and TNA-α (Figure 4C) of both the hydrogel and IOL groups were elevated at the first week post-operation, but that of the hydrogel group stayed consistent with that of the control group at 1 month and 3 months post-operation. In sum, implantation of the poly(acrylamide-co-sodium acrylate) hydrogel did not induce any endophthalmitis in the New Zealand white rabbit eyes.

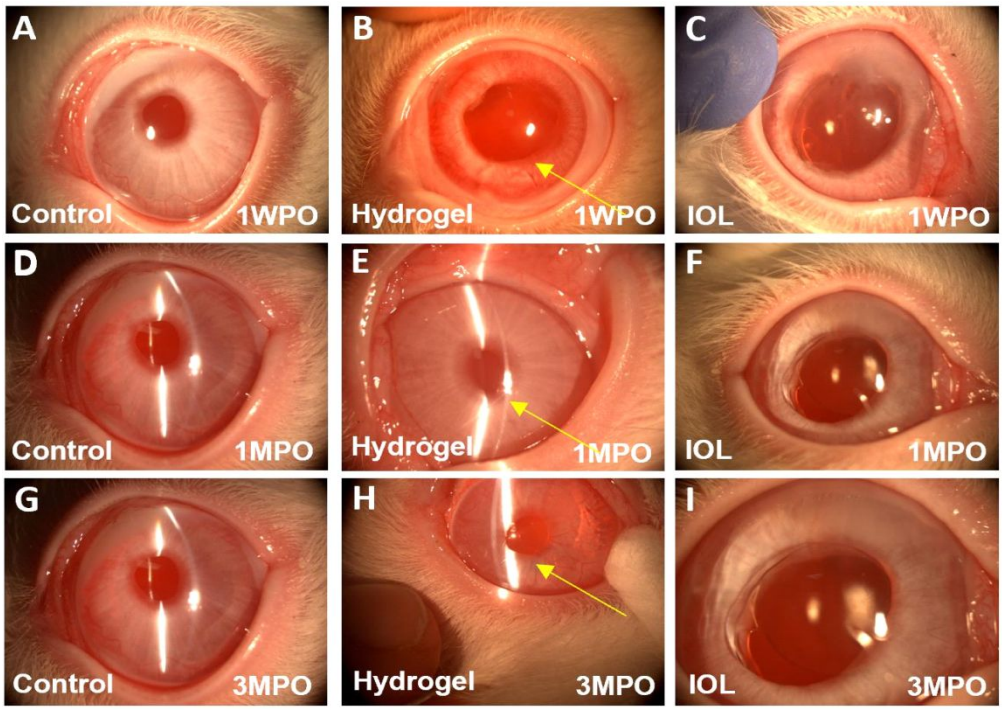

Figure 3 Implantation of poly(acrylamide-co-sodium acrylate) hydrogel thin film into the anterior chamber of New Zealand white rabbits does not induce endophthalmitis

A~C: Slit lamp images of the control group (A), hydrogel group (B) and IOL group (C) at 1 week post-operation showed successful implantation and correct location of the implants; D~F: Slit lamp images of the control group (D), hydrogel group (E) and IOL group (F) at 1 month post-operation showed no significant corneal opacification, keratic precipitate or endophthalmitis; G~I: Slit lamp images of the control group (G), hydrogel group (H) and IOL group (I) at 3 months post-operation showed no significant corneal opacification, keratic precipitate or endophthalmitis. Week post-operation (WPO); Month post-operation (MPO); Yellow arrow: Hydrogel.

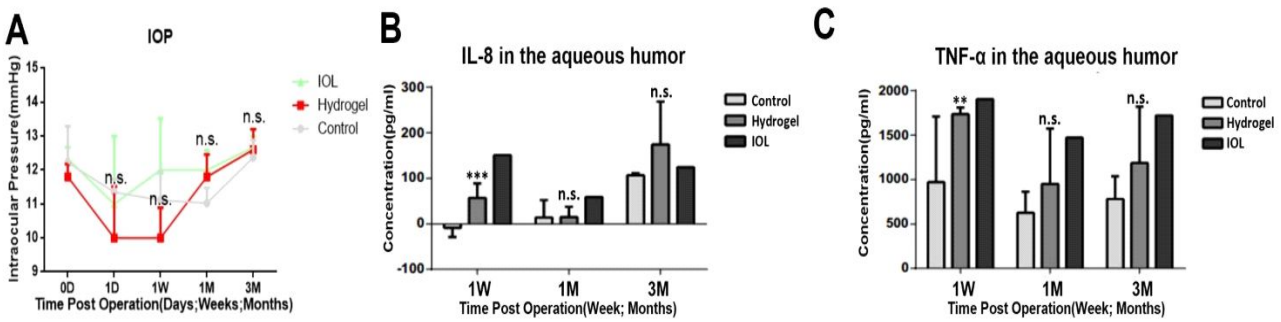

Figure 4 Effects of poly(acrylamide-co-sodium acrylate) hydrogel implantation on the IOP and inflammatory factors in the aqueous humor

A: The IOP recordings revealed showed no significant differences among the control, hydrogel and IOL groups; B~C: ELISA of inflammatory factors such as IL-8 (B) and TNF-α (C) in the aqueous humor of the control, hydrogel and IOL groups; Data are shown as the mean±s.d. Independent sample t test. *$p < 0.05$, **$p < 0.01$; ***$p < 0.005$; n.s. no significance.

Implantation of Poly(Acrylamide-Co-Sodium Acrylate) Hydrogel Does Not Impair Visual Function

Visual function may be well reflected by visual electrophysiology examinations, such as electroretinography (ERG). To further investigate the effect of poly(acrylamide-co-sodium acrylate) hydrogel implantation on visual function, we conducted flash-ERG examinations of the control, hydrogel, and IOL groups. The amplitude of the a-wave of rod, cone and combined rod-cone (Max) ERG 3 months after hydrogel implantation was not significantly altered, nor was the peak time of the wave (Figure 5A, B). Similarly, both the amplitude and peak time of the b-wave of rod, cone and combined rod-cone (Max) ERG 3 months after hydrogel implantation were also not significantly altered (Figure 5C, D). These results indicated normal function of photoreceptor cells and bipolar cells in the hydrogel groups 3 months post-operation. Moreover, we analyzed the characteristics of the Ops wave and light-adapted 30 Hz flicker. Consistent with the results above, the implantation of hydrogel did not affect the amplitude of the Ops wave and light-adapted 30 Hz flicker, as well as its peak time (Figure 5E~G), indicating an intact and well-functioning inner retina and cone system.

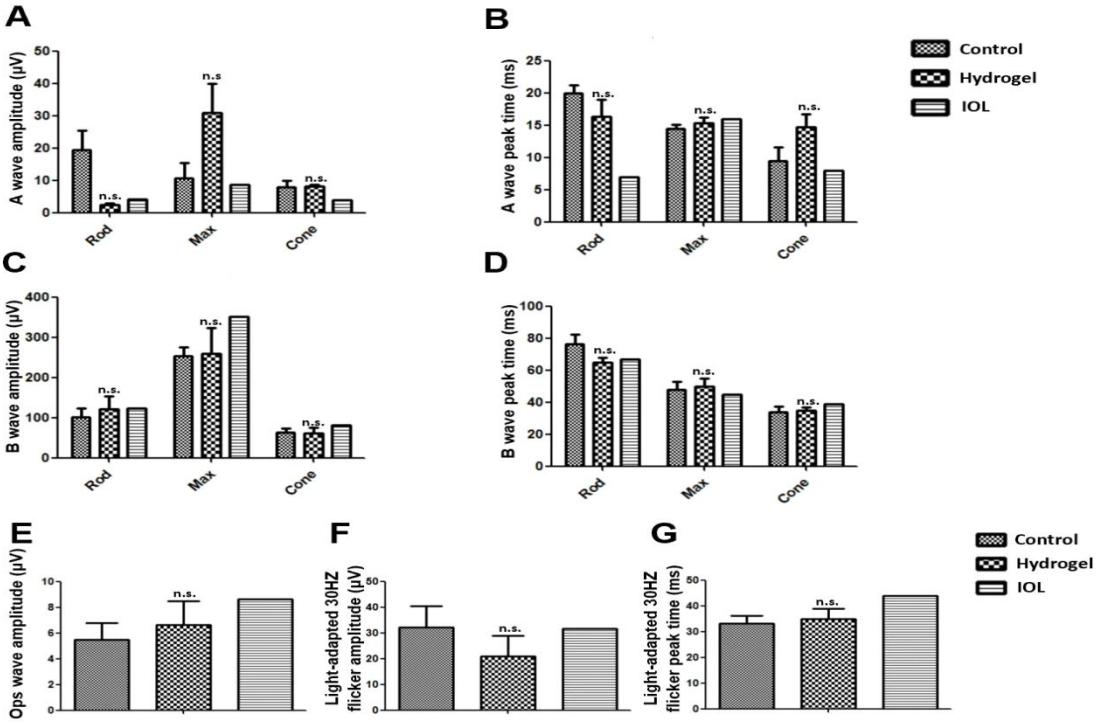

Figure 5 Flash-ERGs of New Zealand white rabbits at 3 months post-implantation

A~B: Statistical analysis of the amplitudes (A) and peak time (B) of fERG a-waves at 0.5 log(cd*s/m^2) in the three groups at 3 months post-operation; C~D: Statistical analysis of the amplitudes (C) and peak time (D) of fERG b-waves at 0.5 log(cd*s/m^2) in the three groups at 3 months post-operation; E~G: Statistical analysis of the Ops wave amplitude (E) at 3.0 log (cd*s/m^2) in the three groups at 3 months post-operation; F~G: Statistical analysis of the light-adapted 30 Hz flicker amplitude (F) and peak time (G) at 3.0 log(cd*s/m^2) in the three groups at 3 months post-operation; Data are shown as the mean±s.d. Independent sample t test. *$p < 0.05$, **$p < 0.01$; ***$p < 0.005$; n.s. no significance.

Implantation of Poly(Acrylamide-Co-Sodium Acrylate) Hydrogel Does Not Damage Ocular Histology

Novel biomaterials are often toxic to the ocular tissue and cause severe abnormalities in histology. To evaluate the effect of poly(acrylamide-co-sodium acrylate) hydrogel implantation on the ocular histology, we first performed HE staining of New Zealand White Rabbit eyes after 3 months of surgery. This result indicated that the hydrogel group maintained its normal histological characteristics, such as cell connections and layered lamination, as well as did the IOL group, all compared with the control group (Figure 6A, B, C). The TUNEL assay revealed that no cellular apoptosis emerged at the cornea, anterior chamber angle (ACA), or retina in any of the three groups, confirming the nontoxic character of the poly(acrylamide-co-sodium acrylate) hydrogel (Figure 7J~R). Moreover, $IBA1^+$ macrophage cells did not accumulate in the cornea or retina except for the ACA in the hydrogel and IOL groups 3 months post-implantation (Figure 7A~I). The recruitment of macrophages at the ACA may represent the immune response caused by the hydrogel or IOL implants, which triggered the phagocytic activation of macrophages.

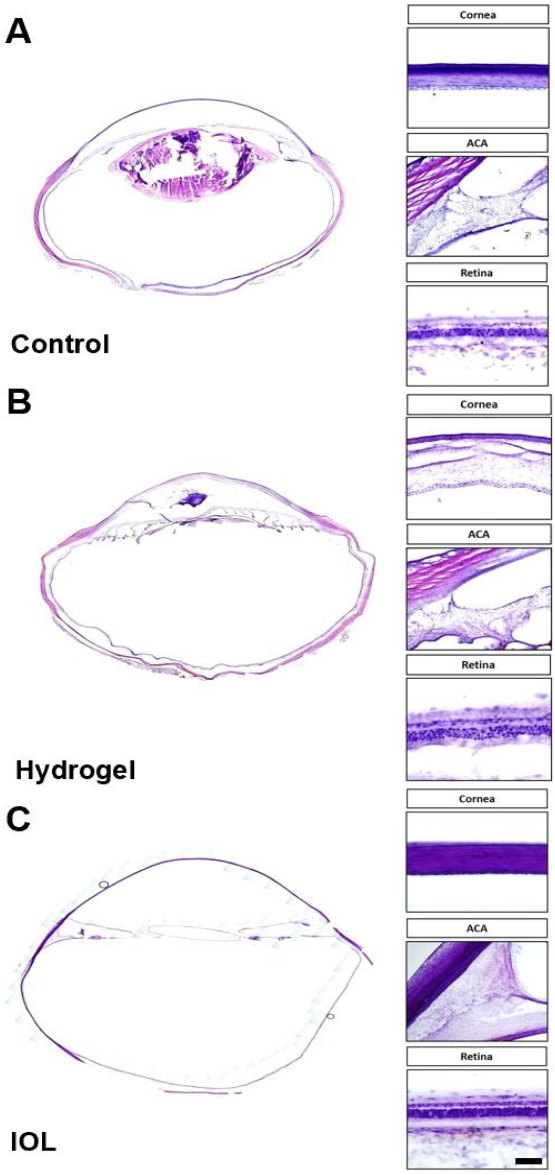

Figure 6 The poly(acrylamide-co-sodium acrylate) hydrogel does not cause histological alteration 3 months post-implantation

A: HE staining of New Zealand White Rabbit eyes showed the detailed histological identity of the cornea, anterior chamber angle, and retina in the control group; B: HE staining of New Zealand White Rabbit eyes showed the detailed histological identity of the cornea, anterior chamber angle, and retina in the hydrogel group. The cell connectivity and layered lamination were normal compared with those of the control group, even though the cornea was ruptured due to the limitations of the HE staining procedure; C: HE staining of New Zealand White Rabbit eyes showed the detailed histological identity of the cornea, anterior chamber angle, and retina in the IOL group. Scale bar, 100 μm.

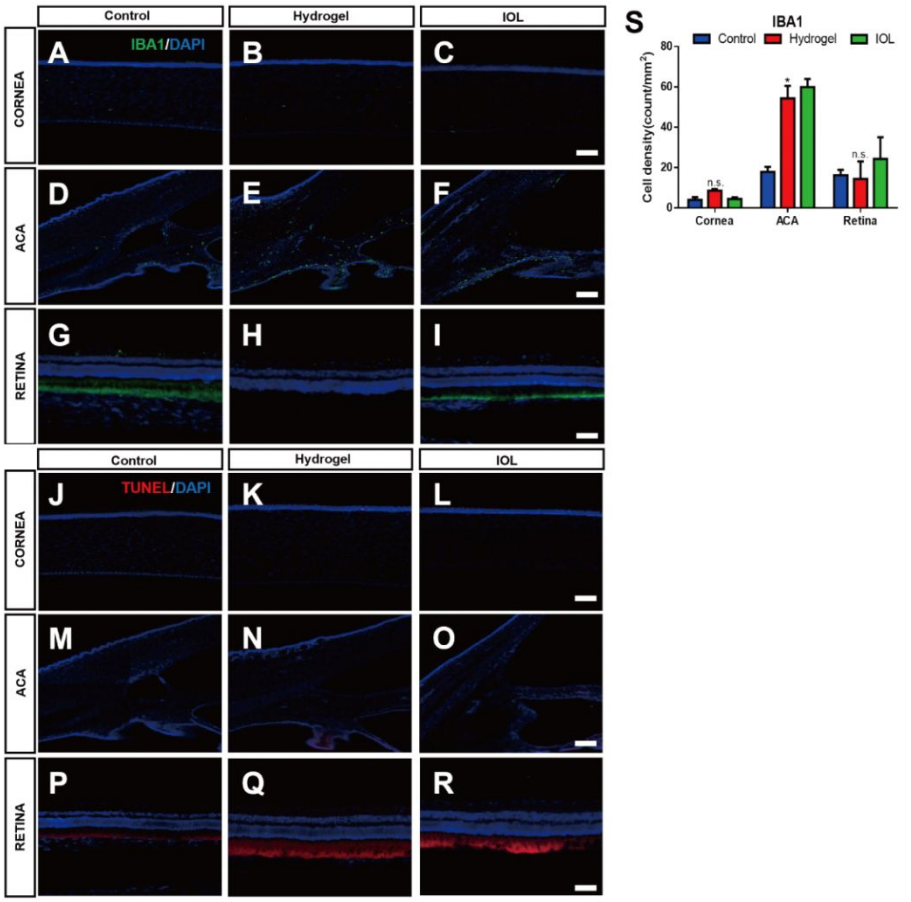

Figure 7 Macrophage activation and cell apoptosis of New Zealand white rabbit eyes 3 months after poly(acrylamide-co-sodium acrylate) hydrogel implantation

A~I: Immunostaining of Iba1 in New Zealand white rabbit eyes at 3 months post-implantation showed Iba1+ macrophage augmentation at the cornea (A~C), ACA (D~F) and retina (G~I) in the control group (A, D, G), the hydrogel group (G, E, H), and the IOL group (C,F,I); J~R: TUNEL assay of New Zealand White Rabbit eyes at 3 months post-implantation showed TUNEL+ apoptotic cell accumulation at the cornea (J~L), ACA (M~O) and retina (P~R) in the control group (J, M, P), the hydrogel group (K, N, Q), and the IOL group (L, O, R); S: Statistical analysis of Iba+ macrophages in the cornea, ANA, and retina in all three groups. Scale bar, 100 μm. Data are shown as the mean±s.d. Independent sample t test. *$p < 0.05$, **$p < 0.01$; ***$p < 0.005$; n.s. no significance.

DISCUSSION

The eye exerts a unique ocular morphology, and all ocular organic architectures are susceptible to a number of diseases that may require treatment via different modalities, such as sustained drug delivery and artificial biotissue substitution.[18] In the past century, hydrogels have been used in various applications as effective materials. The unique network structure of a hydrogel makes it highly hydrophilic and biocompatible, and it exhibits soft physical properties similarly to living tissue, which makes it an ideal and potential biomaterial for ophthalmic applications such as intraocular pumps, injections and implants, reducing comorbidities caused by glaucoma, cataracts, and diabetic retinopathies.[19] 3D printing allows the creation of objects with complex three-dimensional geometries and photologies from a computer-aided design and printed biomaterials to tissue analog structures without any change in their mechanical or biological properties.[20,21] However, given the nature of the polymers in hydrogel formulations and the materials used in the preparation of ophthalmic gels, it is paramount that any new hydrogel formulation intended for ocular application should be inevitably investigated for potential toxicity/adverse effects on ocular tissues. In this report, we generated a poly(acrylamide-co-sodium acrylate) hydrogel as a thin film and found that the newly formed hydrogel needs 9 days of pretreatment with PBS to stabilize its structure, reflecting the stimuli-controlled phase transition and small molecule release characteristics of stimulus-responsive hydrogels[22]. Second, we performed coculture experiments *in vitro* and implantation experiments *in vivo* to assess the effect of the hydrogel on ocular tissue. The biosafety research parameters for structure, function, and inflammation, such as cell proliferation assays, inflammation detection by slit lamp and aqueous humor tests, visual function assay by electroretinogram, and anatomical abnormality detection by HE staining and immunostaining, all indicated that the poly(acrylamide-co-sodium acrylate) hydrogel is qualified as a biosafe clinical-grade biomaterial for 3D-printed IOLs by systematic investigation and verification both *in vivo*

and *in vitro*.

The polymers in preformed ophthalmic hydrogels could be semisynthetic or natural. Some of them can transit from sol to gel conversely triggered by environmental stimuli such as temperature, pH and ion concentration[11,23]. As the poly(acrylamide-co-sodium acrylate) hydrogel was primarily performed by 3D printing, it was harmful to cell proliferation when co-cultured with LECs. (Figure 1C, D). However, pretreatment of the poly(acrylamide-co-sodium acrylate) hydrogel with PBS for 9 days robustly reduced the toxic effect to LECS. This result indicated two points of view: first, the primary poly(acrylamide-co-sodium acrylate) hydrogel could respond to the cell culture environment conditions and release polymers that inhibit cellular proliferation at a high concentration; second, adaptation to the extracellular environment is needed and should be properly investigated and standardized for the safe clinical use of poly(acrylamide-co-sodium acrylate) hydrogels.

When co-cultured with the poly(acrylamide-co-sodium acrylate) hydrogel, both LECs and ARPE19 cells exhibit contact cell death, while cells located far away from the hydrogel grow without any abnormalities. Cell migration and proliferation are highly dependent on the extracellular matrix[24]. To serve as an ideal environment and matrix, ophthalmic hydrogels must be composed of gelatin[25], alginate[26], collagen[27], fibrin[28], and even molecularly modified biomaterials. 3D-printed IOLs have a high light transparency but may be populated by migratory and proliferative cells[29,30]. The contact cell death of the poly(acrylamide-co-sodium acrylate) hydrogel prevented this possibility of this adverse effect of cell migration and proliferation, which makes it an ideal transparent biomaterial with the least opacity after IOL implantation.

A previous study on the ocular tolerability of a new biomaterial formulation used the "Draize rabbit eye irritation test," which is the oldest and most classic test that has been employed to evaluate potential ocular irritation. However, the Draize test is quite limited by its subjectivity, poor reproducibility and the need for large numbers of live rabbits[31,32]. In the current research, we utilized ELISA to explore the inflammatory factor level of the aqueous humor, and we conducted electroretinogram analyses to examine the visual function after hydrogel implantation. These analyses well addressed the shortcomings of the Draize test and provided distinguished data to gain insight into the effect on ocular inflammation and visual function.

Macrophages are a type of immune cell that engulfs and digests debris, foreign substances, and microbes [33]. They are patrol guards in the microenvironment of all tissues, which are transformed into active phagocytes by morphology and function and react quickly to various kinds of tissue damage. There is conclusive evidence in animal models and in situ analysis of human tissues that the macrophage response is a common feature of various retinal inflammatory diseases[34-38]. We found accumulated Iba^+ macrophages in the anterior chamber angle and iris of both hydrogel groups 3 months post-operation. The morphology of Iba^+ macrophages in the anterior chamber angle and iris is ameboid like, suggesting that the phagocytic amoeboid movement of emerging macrophages is triggered by hydrogel implantation. Most importantly, we found similar results in the IOL group, which served as a positive biosafe control group, and no corneal opacity, keratic precipitate, hypopyon, or synechia were observed in the hydrogel or IOL group.

As the implanted IOL will be left in the eye for several years after surgery, there is growing interest in the use of IOLs as drug reservoirs or as treatment methods for ophthalmic diseases. Combining 3D printing technology and the biocompatible poly(acrylamide-co-sodium acrylate) hydrogel as the printing material, as well as a potential material for stimuli-responsive hydrogel fabrication, we hold the possibility of loading antibiotics, corticosteroids, and NSAIDs in the IOL, which integrates cataract surgery and postoperative treatments as a one-step procedure[39]. Moreover, IOLs can also be incorporated with telescopic lenses, presbyopia-correcting lenses, or accommodative polyfocal bioanalogical lenses [40,41]. These advanced designs could become more effective and personalized when combined with 3D printing and biocompatible hydrogels. However, all these IOLs inevitably require rigid biosafety assessments and more clinical studies to ascertain their safety and effectiveness.

In sum, the implantation of the poly(acrylamide-co-sodium acrylate) hydrogel did not disturb the IOP, blood parameters, electroretinogram or optical structure, indicating that it will not cause any ocular irritation. However, it is not clear whether this hydrogel lens maintains the nano smooth surface, which can hopefully to correct visual errors, including the defocusing and astigmatism caused by traditional IOLs. We will improve the manufacturing process in the future and test the correction capacity of this new lens in terms of visual quality. Our research provides insight into the biosafety of poly(acrylamide-co-sodium acrylate) hydrogels in ocular tissue and demonstrates that poly(acrylamide-co-sodium acrylate) hydrogels are a safe material for 3D printing of personal IOLs, which hold great potential for future clinical applications.

REFERENCES:

1 Liu, Y. C., Wilkins, M., Kim, T., Malyugin, B. & Mehta, J. S. Cataracts. *Lancet* **390**, 600-612, doi:10.1016/s0140-6736(17)30544-5 (2017).

2 Allen, D. & Vasavada, A. Cataract and surgery for cataract. *BMJ (Clinical research ed.)* **333**, 128-132, doi:10.1136/bmj.333.7559.128.

3 Kim, T. I., Alió Del Barrio, J. L., Wilkins, M., Cochener, B. & Ang, M. Refractive surgery. *Lancet (London,*

England) **393**, 2085-2098, doi:10.1016/s0140-6736(18)33209-4.
4 Zopf, D. A., Hollister, S. J., Nelson, M. E., Ohye, R. G. & Green, G. E. Bioresorbable airway splint created with a three-dimensional printer. *N. Engl. J. Med.* **368**, 2043-2045, doi:10.1056/NEJMc1206319 (2013).
5 Atala, A., Bauer, S. B., Soker, S., Yoo, J. J. & Retik, A. B. Tissue-engineered autologous bladders for patients needing cystoplasty. *Lancet (London, England)* **367**, 1241-1246, doi:10.1016/s0140-6736(06)68438-9 (2006).
6 Isaacson, A., Swioklo, S. & Connon, C. J. 3D bioprinting of a corneal stroma equivalent. *Exp. Eye Res.* **173**, 188-193, doi:10.1016/j.exer.2018.05.010 (2018).
7 Sommer, A. C. & Blumenthal, E. Z. Implementations of 3D printing in ophthalmology. *Graefe's archive for clinical and experimental ophthalmology = Albrecht von Graefes Archiv fur klinische und experimentelle Ophthalmologie* **257**, 1815-1822, doi:10.1007/s00417-019-04312-3 (2019).
8 Sommer, A. C. & Blumenthal, E. Z. Implementations of 3D printing in ophthalmology. *Graefes Arch. Clin. Exp. Ophthalmol.* **257**, 1815-1822, doi:10.1007/s00417-019-04312-3 (2019).
9 Debellemaniere, G., Flores, M., Montard, M., Delbosc, B. & Saleh, M. Three-dimensional Printing of Optical Lenses and Ophthalmic Surgery: Challenges and Perspectives. *Journal of refractive surgery (Thorofare, N.J. : 1995)* **32**, 201-204, doi:10.3928/1081597x-20160121-05 (2016).
10 Shiblee, M. N. I., Ahmed, K., Khosla, A., Kawakami, M. & Furukawa, H. 3D printing of shape memory hydrogels with tunable mechanical properties. *Soft matter* **14**, 7809-7817, doi:10.1039/c8sm01156g (2018).
11 Al-Kinani, A. A. *et al.* Ophthalmic gels: Past, present and future. *Advanced drug delivery reviews* **126**, 113-126, doi:10.1016/j.addr.2017.12.017 (2018).
12 Hinze, U. *et al.* Implant Design by Means of Multiphoton Polymerization. *Klinische Monatsblatter fur Augenheilkunde* **232**, 1381-1385, doi:10.1055/s-0041-107883 (2015).
13 Chen, X. *et al.* Grafted c-kit+/SSEA1- eye-wall progenitor cells delay retinal degeneration in mice by regulating neural plasticity and forming new graft-to-host synapses. *Stem cell research & therapy* **7**, 191, doi:10.1186/s13287-016-0451-8 (2016).
14 Ullrich M, Aßmus B, Augustin AM, *et al*. SPRED2 deficiency elicits cardiac arrhythmias and premature death via impaired autophagy. *J. Mol. Cell. Cardiol* **129**:13-26, doi: 10.1016/j.yjmcc.2019.01.023 (2019).
15 Lyu X, Ma Y, Wu F, *et al*. LncRNA NKILA Inhibits Retinoblastoma by Downregulating lncRNA XIST. *Curr. Eye Res* **44**(9):975-979, doi: 10.1080/02713683.2019.1606253 (2019).
16 Yu X, Shen N, Zhang ML, *et al*. Egr-1 decreases adipocyte insulin sensitivity by tilting PI3K/Akt and MAPK signal balance in mice. *Embo j*. **30**(18):3754-65, doi: 10.1038/emboj.2011.277 (2011).
17 Liu W, Liu M, Liu Y, *et al*. Validation and Safety of Visual Restoration by Ectopic Expression of Human Melanopsin in Retinal Ganglion Cells. *Hum. Gene Ther*. **30**(6):714-726. doi: 10.1089/hum.2018.009 (2019).
18 Patel, A., Cholkar, K., Agrahari, V. & Mitra, A. K. Ocular drug delivery systems: An overview. *World journal of pharmacology* **2**, 47-64, doi:10.5497/wjp.v2.i2.47 (2013).
19 Koetting, M. C., Peters, J. T., Steichen, S. D. & Peppas, N. A. Stimulus-responsive hydrogels: Theory, modern advances, and applications. *Materials science & engineering. R, Reports : a review journal* **93**, 1-49, doi:10.1016/j.mser.2015.04.001 (2015).
20 Norman, J., Madurawe, R. D., Moore, C. M., Khan, M. A. & Khairuzzaman, A. A new chapter in pharmaceutical manufacturing: 3D-printed drug products. *Advanced drug delivery reviews* **108**, 39-50, doi:10.1016/j.addr.2016.03.001 (2017).
21 Huang, W. & Zhang, X. 3D Printing: Print the future of ophthalmology. *Investigative ophthalmology & visual science* **55**, 5380-5381, doi:10.1167/iovs.14-15231 (2014).
22 Willner, I. Stimuli-Controlled Hydrogels and Their Applications. *Accounts of chemical research* **50**, 657-658, doi:10.1021/acs.accounts.7b00142 (2017).
23 Craig, J. P., Singh, I., Tomlinson, A., Morgan, P. B. & Efron, N. The role of tear physiology in ocular surface temperature. *Eye* **14 (Pt 4)**, 635-641, doi:10.1038/eye.2000.156 (2000).
24 Cope, E. C. & Gould, E. Adult Neurogenesis, Glia, and the Extracellular Matrix. *Cell stem cell* **24**, 690-705, doi:10.1016/j.stem.2019.03.023 (2019).
25 Billiet, T., Gevaert, E., De Schryver, T., Cornelissen, M. & Dubruel, P. The 3D printing of gelatin methacrylamide cell-laden tissue-engineered constructs with high cell viability. *Biomaterials* **35**, 49-62, doi:10.1016/j.biomaterials.2013.09.078 (2014).
26 Duan, B., Hockaday, L. A., Kang, K. H. & Butcher, J. T. 3D bioprinting of heterogeneous aortic valve conduits with alginate/gelatin hydrogels. *Journal of biomedical materials research. Part A* **101**, 1255-1264, doi:10.1002/jbm.a.34420 (2013).
27 Mazzocchi, A., Devarasetty, M., Huntwork, R., Soker, S. & Skardal, A. Optimization of collagen type I-hyaluronan hybrid bioink for 3D bioprinted liver microenvironments. *Biofabrication* **11**, 015003, doi:10.1088/1758-5090/aae543 (2018).
28 Lee, Y. B. *et al.* Bio-printing of collagen and VEGF-releasing fibrin gel scaffolds for neural stem cell culture. *Exp Neurol* **223**, 645-652, doi:10.1016/j.expneurol.2010.02.014 (2010).

29 Buwalda, S. J. & Vermonden, T. Hydrogels for Therapeutic Delivery: Current Developments and Future Directions. **18**, 316-330, doi:10.1021/acs.biomac.6b01604 (2017).
30 Wu, Z. *et al.* Bioprinting three-dimensional cell-laden tissue constructs with controllable degradation. *Scientific reports* **6**, 24474, doi:10.1038/srep24474 (2016).
31 Lordo, R. A., Feder, P. I. & Gettings, S. D. Comparing and evaluating alternative (in vitro) tests on their ability to predict the Draize maximum average score. *Toxicology in vitro : an international journal published in association with BIBRA* **13**, 45-72, doi:10.1016/s0887-2333(98)00062-9 (1999).
32 Abdelkader, H. *et al.* Conjunctival and corneal tolerability assessment of ocular naltrexone niosomes and their ingredients on the hen's egg chorioallantoic membrane and excised bovine cornea models. *International journal of pharmaceutics* **432**, 1-10, doi:10.1016/j.ijpharm.2012.04.063 (2012).
33 Ovchinnikov, D. A. Macrophages in the embryo and beyond: much more than just giant phagocytes. *Genesis (New York, N.Y. : 2000)* **46**, 447-462, doi:10.1002/dvg.20417 (2008).
34 Karlstetter, M. *et al.* Retinal microglia: just bystander or target for therapy? *Prog Retin Eye Res* **45**, 30-57, doi:10.1016/j.preteyeres.2014.11.004 (2015).
35 Rathnasamy, G., Foulds, W. S., Ling, E. A. & Kaur, C. Retinal microglia - A key player in healthy and diseased retina. *Progress in neurobiology* **173**, 18-40, doi:10.1016/j.pneurobio.2018.05.006 (2019).
36 Kanazawa, H., Ohsawa, K., Sasaki, Y., Kohsaka, S. & Imai, Y. Macrophage/microglia-specific protein Iba1 enhances membrane ruffling and Rac activation via phospholipase C-gamma -dependent pathway. *The Journal of biological chemistry* **277**, 20026-20032, doi:10.1074/jbc.M109218200 (2002).
37 Okayasu, T., Quesnel, A. M., O'Malley, J. T., Kamakura, T. & Nadol, J. B., Jr. The Distribution and Prevalence of Macrophages in the Cochlea Following Cochlear Implantation in the Human: An Immunohistochemical Study Using Anti-Iba1 Antibody. *Otology & neurotology : official publication of the American Otological Society, American Neurotology Society [and] European Academy of Otology and Neurotology*, doi:10.1097/mao.0000000000002495 (2019).
38 Cora, M. C. & Janardhan, K. S. Previously Diagnosed Reticulum Cell Hyperplasia in Decalcified Rat Bone Marrow Stain Positive for Ionized Calcium Binding Adapter Molecule 1 (Iba1): A Monocytic/Macrophage Cell Marker. 192623319890610, doi:10.1177/0192623319890610 (2019).
39 Liu, Y. C., Wong, T. T. & Mehta, J. S. Intraocular lens as a drug delivery reservoir. *Curr Opin Ophthalmol* **24**, 53-59, doi:10.1097/ICU.0b013e32835a93fc (2013).
40 Boyer, D., Freund, K. B., Regillo, C., Levy, M. H. & Garg, S. Long-term (60-month) results for the implantable miniature telescope: efficacy and safety outcomes stratified by age in patients with end-stage age-related macular degeneration. *Clin Ophthalmol* **9**, 1099-1107, doi:10.2147/opth.S86208 (2015).
41 Ford, J., Werner, L. & Mamalis, N. Adjustable intraocular lens power technology. *J Cataract Refract Surg* **40**, 1205-1223, doi:10.1016/j.jcrs.2014.05.005 (2014).